Regulation of *O*-glycosylation through Golgi-to-ER relocation of initiation enzymes

David J. Gill,[1] Joanne Chia,[1] Jamie Senewiratne,[1] and Frederic Bard[1,2]

[1]Institute of Molecular and Cell Biology, Proteos, Singapore 138673
[2]National University of Singapore, Singapore 119077

After growth factor stimulation, kinases are activated to regulate multiple aspects of cell physiology. Activated Src is present on Golgi membranes, but its function here remains unclear. We find that Src regulates mucin-type protein *O*-glycosylation through redistribution of the initiating enzymes, polypeptide *N*-acetylgalactosaminyl transferases (GalNac-Ts), from the Golgi to the ER. Redistribution occurs after stimulation with EGF or PDGF in a Src-dependent manner and in cells with constitutively elevated Src activity. All GalNac-T family enzymes tested are affected, whereas multiple other glycosylation enzymes are not displaced from the Golgi. Upon Src activation, the COP-I coat is also redistributed in punctate structures that colocalize with GalNac-Ts and a dominant-negative Arf1 isoform, Arf1(Q71L), efficiently blocks GalNac-T redistribution, indicating that Src activates a COP-I–dependent trafficking event. Finally, Src activation increases *O*-glycosylation initiation as seen by lectin staining and metabolic labeling. We propose that growth factor stimulation regulates *O*-glycosylation initiation in a Src-dependent fashion by GalNac-T redistribution to the ER.

Introduction

Cells respond to external cues, such as growth factor stimulation, by adapting multiple aspects of their physiology. Downstream of cell surface receptors, signaling cascades impact upon protein synthesis, transcriptional programs, cytoskeleton dynamics, and adhesive properties of cells. To regulate these processes, signal transduction complexes associate with specific subcellular structures. Src family kinases (SFKs) form active signaling complexes on Golgi membranes (David-Pfeuty and Nouvian-Dooghe, 1990; Bard et al., 2002; Chiu et al., 2002). We have previously shown that SFKs are important for Golgi structural organization and regulation of COP-I–dependent traffic (Bard et al., 2003); however, the physiological role of Src at the Golgi remains unclear.

One role of the Golgi apparatus is the addition of glycan chains to proteins synthesized through successive addition of simple sugars by various glycosyltransferases. The two main types of glycosylation in the mammalian Golgi apparatus are *N*-glycosylation and *O*-GalNAc glycosylation (referred simply as *O*-glycosylation here). *O*-glycosylation initiation is thought to occur in the Golgi apparatus, although earlier reports had proposed an ER location based on lectin staining (Pathak et al., 1988; Tooze et al., 1988; Perez-Vilar et al., 1991). *O*-glycosylation is initiated by a family of ~20 enzymes called GalNac-Ts, which add *N*-acetyl-galactosamine (GalNAc) to Ser or Thr residues. Most *O*-glycosylation sites can be modified by multiple GalNac-T isoforms, but some isoforms also present site specificity and have different tissue expression patterns (Ten Hagen et al., 2003; Tarp and Clausen, 2008). Consistent with the importance of *O*-glycosylation for metazoans, GalNac-T1 and GalNac-T11 are essential for *Drosophila* embryonic development (Schwientek et al., 2002; Zhang et al., 2008). Similarly, gene knockouts of GalNac-T1 and T3 in mouse result in severe phenotypes (Tenno et al., 2007; Ichikawa et al., 2009). *O*-glycosylation often occurs on several adjacent Ser or Thr, especially in mucin proteins and, by contrast with *N*-glycosylation, there is no consensus sequence identified for GalNAc addition. Several glycosyltransferases act after GalNac-Ts in a stepwise manner to form a complex array of *O*-linked glycan structures (Spiro, 2002; Freeze, 2006). *O*-glycosylation sites as well as *O*-glycan structures

Correspondence to Frederic Bard: fbard@imcb.a-star.edu.sg

Abbreviations used in this paper: Arf1, ADP ribosylation factor 1; COP-I, coat protein complex I; ERGIC, ER-to-Golgi intermediate compartment; GalNAc, *N*-acetyl-galactosamine; GalNac-T, polypeptide *N*-acetylgalactosaminyl transferase; GalT, β 1,4-galactosyltransferase; HPL, *Helix pomatia* lectin; ManII, Mannosidase II; PDI, protein disulphide isomerase; SFK, SRC family kinase; SKI, Src kinase inhibitor; SYF, Src/Yes/Fyn depleted.

© 2010 Gill et al. This article is distributed under the terms of an Attribution–Noncommercial–Share Alike–No Mirror Sites license for the first six months after the publication date (see http://www.rupress.org/terms). After six months it is available under a Creative Commons License (Attribution–Noncommercial–Share Alike 3.0 Unported license, as described at http://creativecommons.org/licenses/by-nc-sa/3.0/).

The Rockefeller University Press $30.00
J. Cell Biol. Vol. 189 No. 5 843–858
www.jcb.org/cgi/doi/10.1083/jcb.201003055

vary dramatically between tissues (Hanisch, 2001), during inflammation (Crocker and Redelinghuys, 2008) and in cancer (Brockhausen, 2006). Regulation of *O*-glycosylation initiation is thought to depend mostly on the expression levels of GalNac-Ts. These variations are likely to carry a physiological importance as *O*-glycosylation can increase substantially the hydrophilicity and turgidity of cell surface glycoproteins and can affect the adhesive properties of cells. *O*-glycosylation also creates binding sites for glycoproteins, for example, selectins that mediate binding of leukocytes to endothelial cells (Ley and Kansas, 2004; Hang and Bertozzi, 2005).

Here, we investigated the effect of Src activation on localization of various Golgi proteins and find that Src induces Golgi-to-ER retrograde trafficking of *O*-glycosylation initiation enzymes GalNac-Ts via a COP-I–dependent mechanism. This relocation dramatically increases protein *O*-glycosylation initiation.

Results

Growth hormone stimulation redistributes GalNac-T1 from the Golgi apparatus

We have previously investigated the role of Src at the Golgi by comparing cell lines with different levels of Src expression (Bard et al., 2003). In normal cells, Src can be activated downstream of various growth factor receptors, such as EGF or PDGF receptors (Thomas and Brugge, 1997). To investigate whether such stimulation could affect Golgi physiology, we compared staining patterns of various Golgi markers in serum-starved HeLa cells with those further stimulated with EGF. The *Helix pomatia* lectin (HPL) marks Golgi membranes under usual growing conditions (10% FBS). Upon serum starvation, this staining pattern is not significantly affected (Fig. 1 A and Fig. S1, A and B). By contrast, upon EGF stimulation, HPL staining is significantly redistributed from its perinuclear localization while the Golgi marker Giantin is unaffected (Fig. 1 B). Similar results were obtained upon PDGF stimulation (Fig. S1 C). To quantify redistribution of HPL, the ratio of staining between the Golgi and neighboring cytoplasm was compared using a method outlined in Fig. 1 C and the amount of HPL staining at the Golgi was found to decrease progressively with longer EGF stimulation (Fig. 1 D). HPL binds various glycans but in particular to terminal α-linked *N*-acetyl galactosamine residues (GalNAc) linked to Ser or Thr residues (Sanchez et al., 2006). This structure is also known as the Tn antigen. To verify that HPL staining indeed reflects mostly GalNAcs α-linked to proteins in our various experimental conditions, we compared anti-Tn antibody and HPL stainings and found that they colocalize at the Golgi before stimulation (Fig. 1 E) and are redistributed upon stimulation with EGF (Fig. 1 F). Identical results were obtained after stimulation with PDGF (Fig. S1, D and E).

GalNAc is added onto proteins by GalNac-Ts (Ten Hagen et al., 2003). Consequently, redistribution of anti-Tn and HPL staining by growth factor addition is likely due to relocation of GalNac-Ts normally localized at the Golgi apparatus (Röttger et al., 1998). Indeed, in unstimulated HeLa cells, GalNac-T1 and HPL colocalize exclusively at the Giantin-stained Golgi apparatus (Fig. 2 A), whereas after EGF treatment a significant amount of GalNac-T1 staining is apparent in punctate and diffuse cellular structures that stain positively for HPL (Fig. 2 B). Similar results were obtained upon PDGF stimulation (Fig. S1 F). Consistent with the idea that GalNac-T1 is redistributed away from the Golgi apparatus, when using constant image acquisition parameters, the amount of GalNac-T1 at the Giantin-stained Golgi is significantly decreased after 4 h of EGF treatment (Fig. 2 C). Quantification of the ratio of Golgi/neighboring cytosol staining averaged over multiple cells confirmed that the amount of GalNac-T1 at the Golgi decreases progressively with longer EGF stimulation time (Fig. 2 D). Growth factor stimulation can alter cell physiology through changes in gene expression; however, addition of α-Amanitin (a potent inhibitor of RNA polymerase II) does not prevent redistribution of HPL staining under EGF stimulation (Fig. S2), indicating that HPL staining redistribution is independent of transcription and more likely due to membrane trafficking events.

GalNac-T1 redistribution is dependent on Src activation

We next investigated whether Src activation was important for GalNac-T redistribution by treating HeLa cells with EGF and 10 μM of Src kinase inhibitors (SU6656 or Src kinase inhibitor 1 [SKI]; (Fig. 3 A). In cells without Src inhibitor treatment (DMSO only), the ratio of Golgi-specific HPL labeling dropped from fivefold to twofold after 4 h of EGF stimulation (Fig. 3, A and B). Strikingly, HPL redistribution was completely or partially blocked in cells treated with 10 μM SKI or SU6656, respectively, as apparent visually and after quantification (Fig. 3, A and B). Similar results were obtained upon inhibition of Src with 10 μM SKI after PDGF stimulation (Fig. 3 C). Src activity can also be up-regulated, for example in human breast cancer cells, by an increase in its expression levels (Ottenhoff-Kalff et al., 1992). As a model of such constitutive activation, we compared mouse fibroblast cell lines with different levels of Src activity: SYF, lacking Src/Yes/Fyn (ubiquitous SFKs), and SYFsrc, where Src has been reintroduced into SYF cells and is overexpressed threefold relative to normal fibroblasts (Klinghoffer et al., 1999). At low resolution, HPL staining has a perinuclear distribution in SYF cells, which is similar to most fibroblast cell lines tested. By contrast, a reticulated network is prevalent in SYFsrc cells (Fig. 3 D). At higher resolution, HPL staining colocalizes exclusively with Mannosidase II (ManII)–stained Golgi membranes in SYF cells, whereas in SYFsrc cells, a reticulated network with punctate structures is also apparent (Fig. 3 E). In addition, significant additional redistribution of HPL staining from the Giantin-stained Golgi apparatus was observed in SYFsrc cells and not in SYF cells stimulated with EGF or PDGF for 2 h (Fig. S3). Finally, to test whether Src can directly perturb GalNac-T localization, an active Src mutant tagged at its C terminus with DsRed (SrcE-DsRed, containing the activating E378G mutation) and a GFP-tagged form of Mannosidase II (ManII-GFP) were microinjected in human WI38 fibroblasts (cells that stain well for several GalNac-Ts). Soon after Src became detectable (~3 h after microinjection), the perinuclear Golgi staining of GalNac-T1 was significantly decreased in microinjected cells, whereas the Golgi delineated by ManII-GFP remained normal,

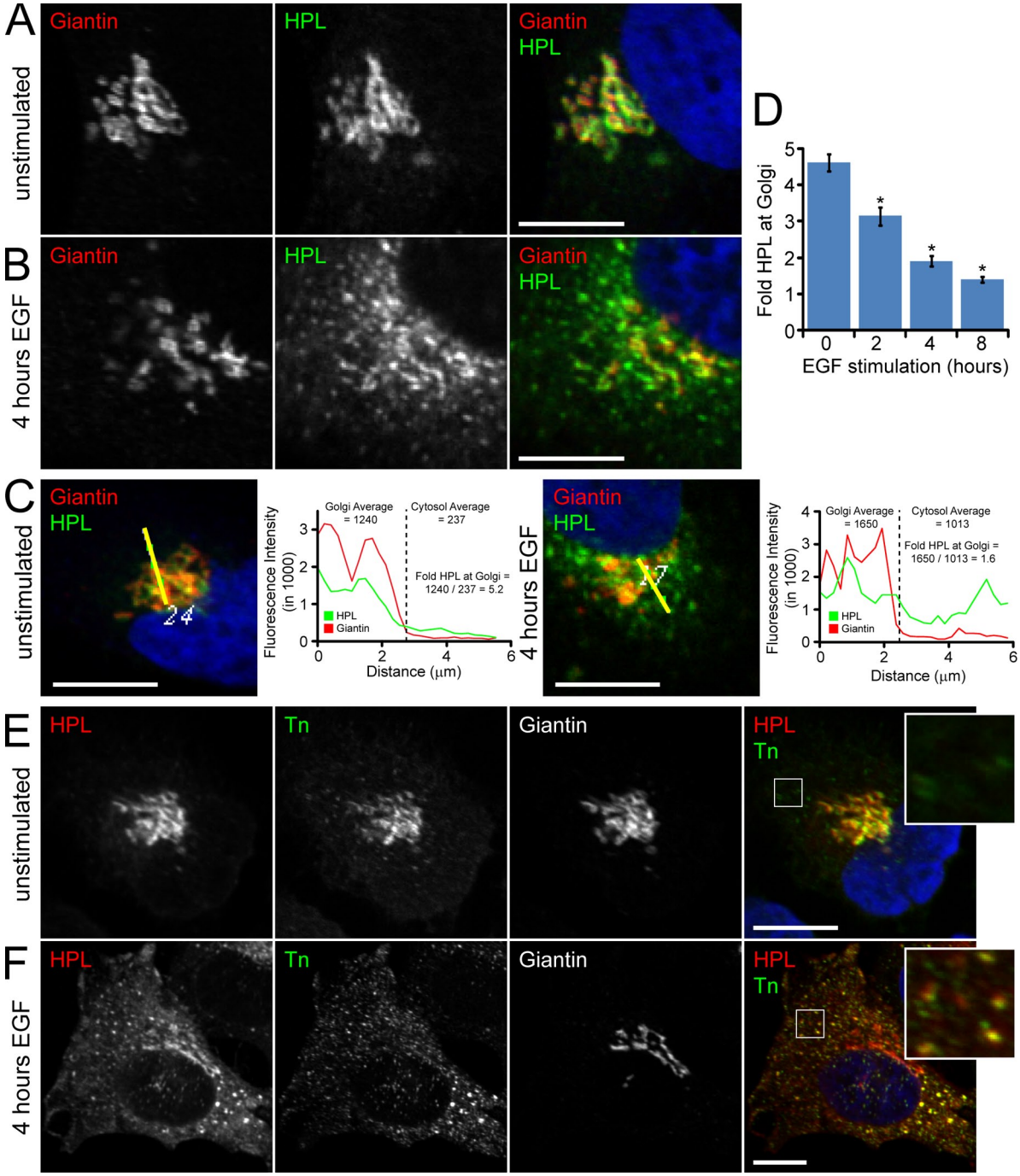

Figure 1. **Growth factor stimulation effect on *O*-glycosylation marker distribution.** (A and B) *Helix pomatia* lectin (HPL) staining at the Golgi (Giantin) in unstimulated HeLa cells (A) is redistributed out of the Golgi after EGF treatment (100 ng/ml) for 4 h (B). (C) HPL staining at the Golgi or neighboring cytoplasm is measured to quantify the fold enrichment at the Golgi. (D) HPL enrichment at the Golgi progressively decreases with increased EGF stimulation. 30 cells were quantified for each sample. Error bars show SEM. Statistical significance (p) measured by two-tailed paired *t* test. *, $P < 0.001$ relative to mean HPL staining in unstimulated cells (0 h). This is a representative example from three independent experiments. (E and F) Anti-Tn staining colocalizes with HPL at the Golgi in unstimulated HeLa cells (E) or away from the Golgi in punctate cytoplasmic structures after EGF treatment for 4 h (F). In all images nuclei were stained using Hoechst and colored blue. Bar, 10 μm.

highlighting that Src can directly and rapidly induce GalNac-T redistribution from the Golgi apparatus (Fig. S4 A).

Several GalNac-Ts redistribute away from the Golgi apparatus

Although GalNac-T1 is a major and ubiquitous member of the family, GalNac-Ts form a family of ~20 enzymes (Ten Hagen et al., 2003; Tarp and Clausen, 2008). To test whether other GalNac-Ts were redistributed from the Golgi upon Src activation, we used Src(E378G) microinjection in WI38 human fibroblasts as it induces a clear and strong redistribution of GalNac-T1 without significant Golgi perturbation. Indeed, when Src activity is very high, such as after microinjection or transient transfection of an activated kinase, some cell lines such as HeLa

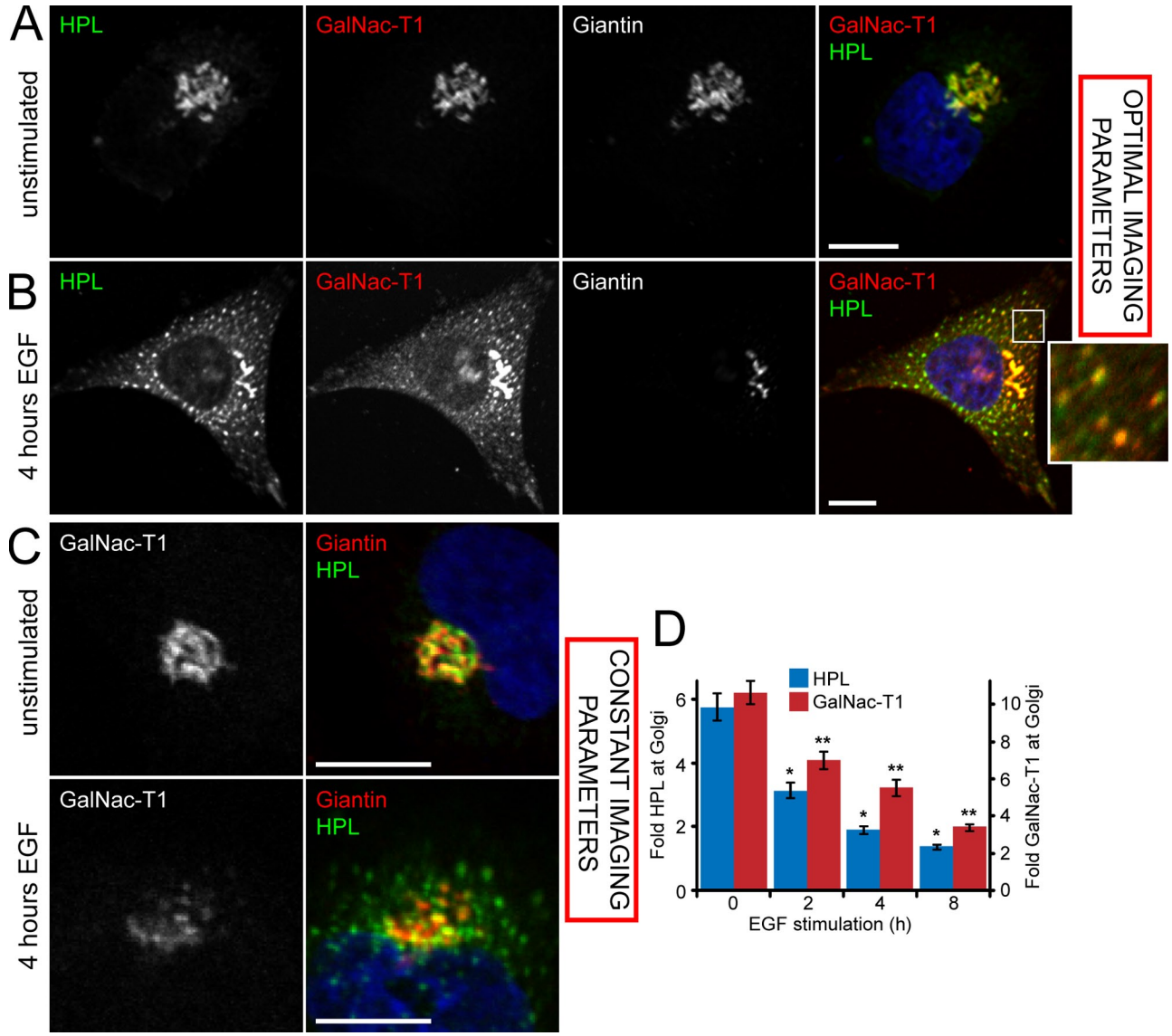

Figure 2. **Src activation redistributes GalNac-T1 from the Golgi.** (A and B) GalNac-T1 and HPL staining colocalizes only at the Golgi (Giantin) in unstimulated HeLa cells (A) but also in punctate cytoplasmic structures after EGF treatment (100 ng/ml) for 4 h (B). (C) The amount of GalNac-T1 staining colocalizing with Golgi membranes was compared between unstimulated HeLa cells and 4 h EGF-treated HeLa cells using fixed laser power and detector voltages. (D) Quantification of GalNac-T1 and HPL enrichment at the Golgi in HeLa cells treated with EGF for indicated times. 30 cells were quantified for each sample. Error bars show SEM. Statistical significance (p) measured by two-tailed paired *t* test. * and **, $P < 0.001$ relative to mean HPL or GalNac-T1 staining, respectively, in unstimulated cells (0 h). This is a representative example from three independent experiments. In all images nuclei were stained using Hoechst and colored blue. Bar, 10 µm.

suffer a significant fragmentation of the whole Golgi apparatus. All GalNac-Ts tested (T1, T2, T3, T4, and T6) were redistributed in this assay (Fig. S4, A–C; and unpublished data). By contrast, our initial screen on Src effect on Golgi markers had revealed that other Golgi enzymes, such as ManII and β4-galatosyltransferase, are not redistributed after Src activation (Fig. S5). GalNac-Ts have been proposed to be present in the cis-Golgi cisternae (Roth et al., 1994), whereas the two previous enzymes are respectively medial and trans located. However, a known cis-Golgi enzyme, α-1,2-mannosidase IC (ManIC), as well as the cis-Golgi marker GM130, were also not affected, indicating that cisternal localization alone cannot explain the specific redistribution of GalNac-Ts. Src expression also had no visible effect on the intracellular distribution of glucosaminyl *N*-acetyl transferase 1 core 2 (C2GnT), an enzyme that functions downstream of the GalNac-Ts (Fig. S5), suggesting that the *O*-glycosylation pathway is only targeted at the level of the initiation enzymes. A summary of all the Golgi markers tested and their results is presented in Table I.

Src activation redistributes GalNac-Ts from the Golgi to the ER

In both EGF-stimulated HeLa cells and activated Src SYFsrc fibroblasts, HPL appears to stain a reticulated network reminiscent of the ER and punctate structures distributed throughout the cytoplasm reminiscent of the ER-to-Golgi intermediate compartment (ERGIC; Figs. 1 B and 3 E). Consistently, while in unstimulated HeLa cells GalNac-T1 localizes in the perinuclear Golgi

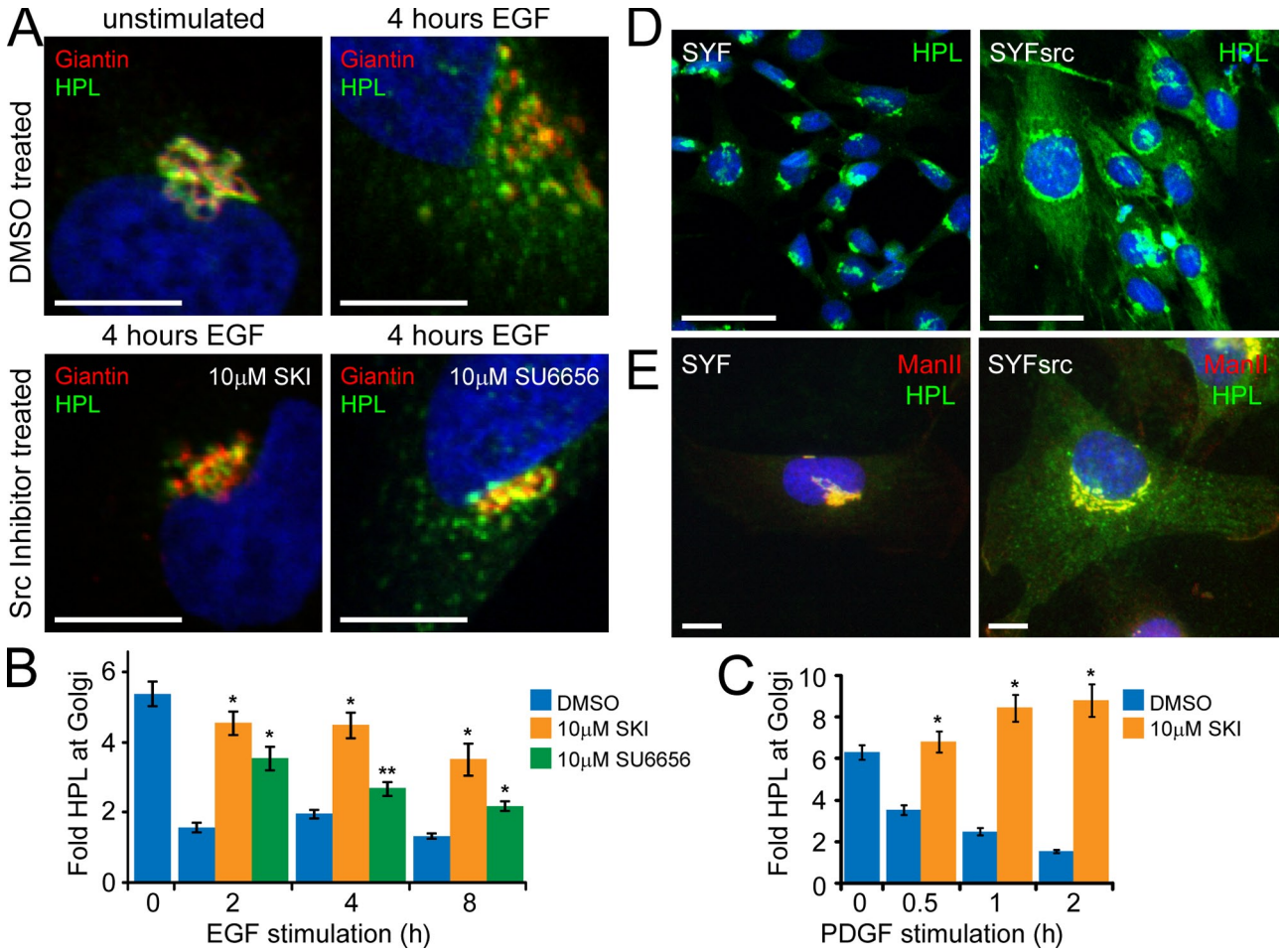

Figure 3. **Redistribution of GalNac-Ts from the Golgi is dependent on Src activity levels.** (A) HPL staining redistributed out of the Golgi (Giantin) in HeLa cells upon EGF stimulation (100 ng/ml) for 4 h is inhibited with cotreatment of 10 μM Src kinase inhibitors SKI and SU6656. (B) Quantification of HPL enrichment at the Golgi in HeLa cells cotreated with EGF and either DMSO or 10 μM Src inhibitors (SKI, SU6656) for indicated times. 30 cells were quantified for each sample. Error bars show SEM. Statistical significance (p) measured by two-tailed paired *t* test. * or **, $P < 0.001$ or $P < 0.05$, respectively, relative to mean HPL staining in DMSO-treated cells at each time point. This is a representative example from two independent experiments. (C) Quantification of HPL enrichment at the Golgi in HeLa cells cotreated with PDGF (50 ng/ml) and either DMSO or 10 μM SKI for indicated times. 30 cells were quantified for each sample. Error bars show SEM. Statistical significance (p) measured by two-tailed paired *t* test. *, $P < 0.001$ relative to mean HPL staining in DMSO-treated cells at each time point. This is a representative example from two independent experiments. (D) Low resolution immunofluorescence studies of HPL staining highlighting a reticulated network only in Src-activated SYFsrc fibroblasts and not Src-deficient SYF fibroblasts. (E) High resolution immunofluorescence studies of HPL and Mannosidase II staining in Src-deficient SYF and Src-activated SYFsrc fibroblasts. In all images nuclei were stained using Hoechst and colored blue. Bars: (A and E) 10 μm; (D) 50 μm.

(Fig. 4 A), after EGF treatment it colocalizes with ERGIC53 in punctate structures distributed throughout the cell (Fig. 4 B). Similarly, anti-Tn staining colocalizes with ERGIC53-positive punctate structures only in EGF-stimulated HeLa cells (not depicted). Due to weak antibody staining, visualization of GalNac-Ts in the ER is arduous but HPL and anti-Tn staining can both be found colocalizing with the ER protein markers PDI (protein disulphide isomerase) and calreticulin, respectively (Fig. 4, C and D; and unpublished data). These results indicate that GalNac-Ts are being relocalized to the ER and the ERGIC under conditions of Src activation.

To probe for GalNac-Ts in the ER, an ER-trapped reporter for GalNac-T activity (Muc-PTS) containing a proline, threonine, and serine (PTS)–rich sequence from the Muc5AC mucin was constructed (Fig. 5 A). This reporter contains up to 15 sites of GalNAc addition, as well as a secretion signal sequence fused to GFP at its N terminus and a KDEL motif at its C terminus to enable its delivery and retention in the ER. Muc-PTS targeting to the ER and not the Golgi was verified under both active and inactive Src-expressing conditions by costaining with the ER and Golgi markers PDI and Giantin, respectively (Fig. 5, B–E). Muc-PTS glycosylation status could be evaluated either by a size shift on gel after immunoprecipitation (due to both the added molecular weight of GalNAc residues and reduced binding to SDS; Fukuda and Tsuboi, 1999) or by its binding to HPL agarose beads. To verify that Muc-PTS glycosylation in the ER could be detected, a constitutively ER-targeted form of GalNac-T2 (abbreviated ER-GALNT2) was constructed by fusing GalNac-T2 to the cytosolic tail of the ER resident MHC class II protein p33 (Röttger et al., 1998). As a control, ER-GALNT2 containing the H226D mutation, which completely abrogates its catalytic activity (Fritz et al., 2004), was also generated. After coexpression with active ER-GALNT2 in HEK293T cells, the apparent molecular size of Muc-PTS was higher (45–55 kD) than when expressed

Table I. **Effect of Src activation on redistribution of Golgi resident proteins**

Golgi proteins tested	Redistributed to ER under EGF stimulation (HeLa cells)	Redistributed to ER under Src microinjection (either mouse SYF or human WI38 fibroblasts)
Structural proteins		
Giantin	−	NT
Glycosyltransferases		
Mannosidase II	−	− (SYF)
Mannosidase IC[a]	NT	− (SYF)
β4-GALT[b]	NT	− (SYF)
C2GnT[c]	NT	− (SYF)
GalNac-T1	++	++ (WI38)
GalNac-T2	++	++ (WI38)
GalNac-T3	++	++ (WI38)
GalNac-T4	NT	++ (WI38)
GalNac-T6	NT	++ (WI38)
COP-I regulatory proteins		
Arf1[d]	++	++ (SYF)
COP-I β1	++	++ (SYF)
COP-I γ1	++	NT

−, not affected; ++, strong redistribution; NT, not tested.

[a]Transfection of full-length Mannosidase IC tagged at its N terminus with an HA tag.

[b]Transfection of β4-GALT GFP-tagged reporter construct.

[c]Transfection of full-length C2GnT tagged at its C terminus with a DsRed tag.

[d]Transfection of full-length Arf1 tagged at its C terminus with a GFP or a V5 tag.

alone or with inactive ER-GALNT2(H226D) (~45 kD; Fig. 5 F). In addition, a significant increase of Muc-PTS binding to HPL resin was observed when Muc-PTS was coexpressed with active ER-GALNT2, demonstrating that it is significantly glycosylated only when active GalNac-Ts are present in the ER.

Muc-PTS was next used to monitor the apparition of endogenous GalNac-T activity in the ER upon Src activation. Muc-PTS was transfected into HEK293T cells 36 h before overnight serum starvation and subsequent EGF stimulation to activate Src. After 2–4 h of EGF stimulation, the extent of GalNAc modification in Muc-PTS was substantially higher as judged by increased binding to HPL agarose (Fig. 5 G). Similarly, only active Src and not inactive Src could promote GalNac-T activity in the ER when Muc-PTS was cotransfected with Src expression plasmids as seen by both anti-FLAG immunoprecipitation and HPL pull-down (Fig. 5 H). In the active Src-expressing conditions, a significant fraction of Muc-PTS had a shifted apparent molecular size (up to 55 kD) similar to the shift observed with ER-targeted GalNac-T2 (Fig. 5, F and H). This is consistent with our immunofluorescence results indicating more extensive GalNac-T redistribution upon expression of an active Src than upon EGF stimulation.

Src activation induces COP-I staining redistribution

Golgi-to-ER retrograde traffic of several proteins such as the KDEL-R has been shown to depend upon COP-I vesicles. The COP-I coat is built from several subunits and is thought to provide a force to sort cargo into transport intermediates (Hsu et al., 2009). Golgi enzymes have been shown to be enriched in COP-I vesicles in some conditions (Lanoix et al., 2001; Malsam et al., 2005). Our previous work indicated that Src regulates COP-I vesicular traffic (Bard et al., 2003). Together, this suggests that GalNac-T redistribution to the ER upon Src activation could be mediated by COP-I vesicles. Consistently, upon EGF activation, the distribution of two coat components, β1 and γ1, were redistributed from the Golgi apparatus to punctate structures distributed throughout the cell and reminiscent of the ERGIC (Fig. 6, A and B). Before EGF stimulation, GalNac-T1 colocalizes exclusively with β1 and γ1 COP-I coat components at HPL-stained Golgi membranes (Fig. 6, C and E). By contrast, after EGF stimulation GalNac-Ts also colocalize partially with β1 and γ1 COP-I coat components in the new punctate structures (Fig. 6, D and F). These data suggest that GalNAc-Ts are being redistributed from the Golgi apparatus to the ER by a process that requires COP-I vesicles.

Arf1 activity is required for GalNac-T redistribution

Arf proteins are well-characterized regulators of COP-I vesicle biogenesis (for review see D'Souza-Schorey and Chavrier, 2006). Preliminary experiments indicated that expression of active Src(E378G) in Src-deficient SYF cells reduces Arf1 levels on Golgi membranes (unpublished data). Exogenously expressed Arf1-GFP at the Golgi in serum-starved HeLa cells was redistributed to punctate cytoplasmic structures after EGF stimulation (Fig. 7, A and B). To test Arf1 function in GalNac-T redistribution, we used the constitutively active mutant Arf1(Q71L), which blocks the final stages of COP-I vesicle biogenesis at the Golgi due to its inability to hydrolyze bound GTP into GDP (Dascher and Balch, 1994). Expression of wild-type Arf1-GFP and Arf1(Q71L)-GFP alone does not perturb GalNac-T location in unstimulated HeLa cells, as indicated by HPL staining concentrated at the Golgi (Fig. 7 A). After EGF stimulation for 4 h, HPL staining in wild-type Arf1-GFP–expressing HeLa cells was dispersed in a fashion similar to untransfected cells (Fig. 7 B). By contrast, Arf1(Q71L)-GFP–expressing HeLa cells displayed less HPL dispersion with a significant amount remaining colocalized with Giantin-stained Golgi membranes (Fig. 7 B). Quantification of HPL Golgi staining during EGF stimulation revealed a slower rate of decrease with Arf1(Q71L)-GFP at all times (Fig. 7 C). Arf1(Q71L)-GFP also blocked HPL redistribution under expression of active Src(E378G)-DsRed (SrcE-DsRed) in Src-deficient SYF fibroblasts (Fig. 7, D and E). Interestingly, when Arf1 function is inhibited, active Src accumulates more readily at the Golgi (Fig. 7 E). As a control for these studies, we found that coexpression of inactive Src (SrcK-DsRed) with wild-type Arf1 does not promote redistribution of GalNac-Ts, indicated by HPL staining enriched at the Golgi (Fig. 7 F). Altogether, these results show that Arf(Q71L) but not wild-type Arf1 can block or delay the trafficking of GalNAc-Ts to the ER induced by Src. To directly test the effect of Arf(Q71L) on the redistribution of GalNAc-Ts, we used the ER-trapped Muc-PTS glycosylation reporter. As judged by the smaller apparent size and less efficient pull-down using HPL, the extent of Muc-PTS GalNAc glycosylation was much lower in cells where Arf1(Q71L) but not wild-type Arf1 was coexpressed with

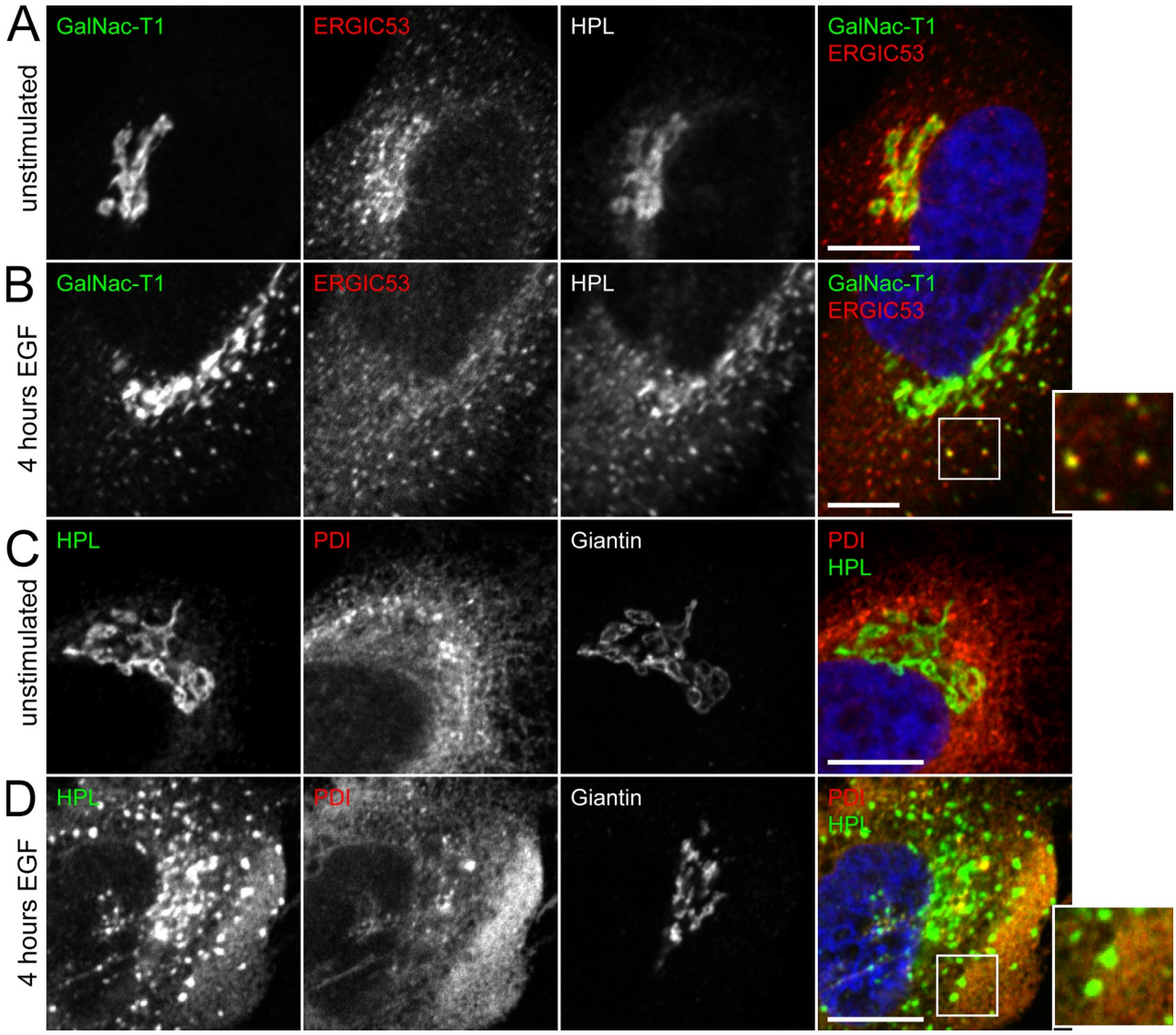

Figure 4. **GalNac-Ts are trafficked to ERGIC and ER compartments upon Src activation.** (A) GalNac-T1 and ERGIC53 staining colocalizes moderately only at the Golgi apparatus (Giantin) in unstimulated HeLa cells. (B) GalNac-T1 and ERGIC53 staining colocalizes in novel punctate ER-to-Golgi intermediate compartment (ERGIC) structures upon EGF treatment (100 ng/ml) for 4 h. These structures stain positively for HPL. (C) HPL staining is present exclusively at the Golgi with no significant colocalization with ER marker (PDI) in unstimulated HeLa cells. (D) HPL staining is present in diffuse structures that stained with an ER marker (PDI) upon EGF treatment for 4 h. In all images nuclei were stained using Hoechst and colored blue. Bar, 10 µm.

active Src (SrcE; Fig. 7 G). Overall, these results demonstrate that Arf1 is critical for mediating trafficking of GalNAc-Ts to the ER upon Src activation. Together with our results on COP-I staining, this strongly suggests that GalNAc-Ts are redistributed from the Golgi to the ER by COP-I vesicles.

O-glycosylation initiation is up-regulated upon Src activation

We hypothesized that redistribution of GalNac-Ts from the Golgi to the ER could significantly increase total *O*-glycosylation initiation by exposing protein substrates to GalNac-Ts earlier and for a longer time. Consistent with this idea, total cellular HPL staining intensity increases 2.1-fold between Src-deficient SYF cells and activated Src SYFsrc cells, and 2.5-fold between basal Src NIH3T3 cells and activated Src NIH3T3-vsrc cells (Fig. 8 A). In addition, we also observed a 2- and 1.8-fold increase in total HPL staining in HeLa cells treated for 3 h with EGF and PDGF, respectively, relative to unstimulated serum-starved cells (Fig. 8 B). To independently verify this increase of *O*-glycosylation initiation, we metabolically labeled cells with GalNAz, a GalNAc analogue that can be incorporated into proteins by GalNac-Ts and, after cell lysis, specifically labeled with a FLAG epitope (Laughlin and Bertozzi, 2007). When SYF and SYFsrc cells are GalNAz labeled for 24 h and similar amounts of total cell lysate are analyzed using anti-FLAG Western blot, SYFsrc cells display significantly higher GalNAz labeling of various proteins (Fig. 8 C). Similarly, EGF stimulation of serum-starved HeLa cells results in higher GalNAz incorporation after 2 h and more significantly after 4 h (Fig. 8 D). The Western blot patterns indicate that multiple proteins have an increased incorporation of GalNAz, suggesting that the propensity of various residues in various proteins to become *O*-glycosylated increases significantly

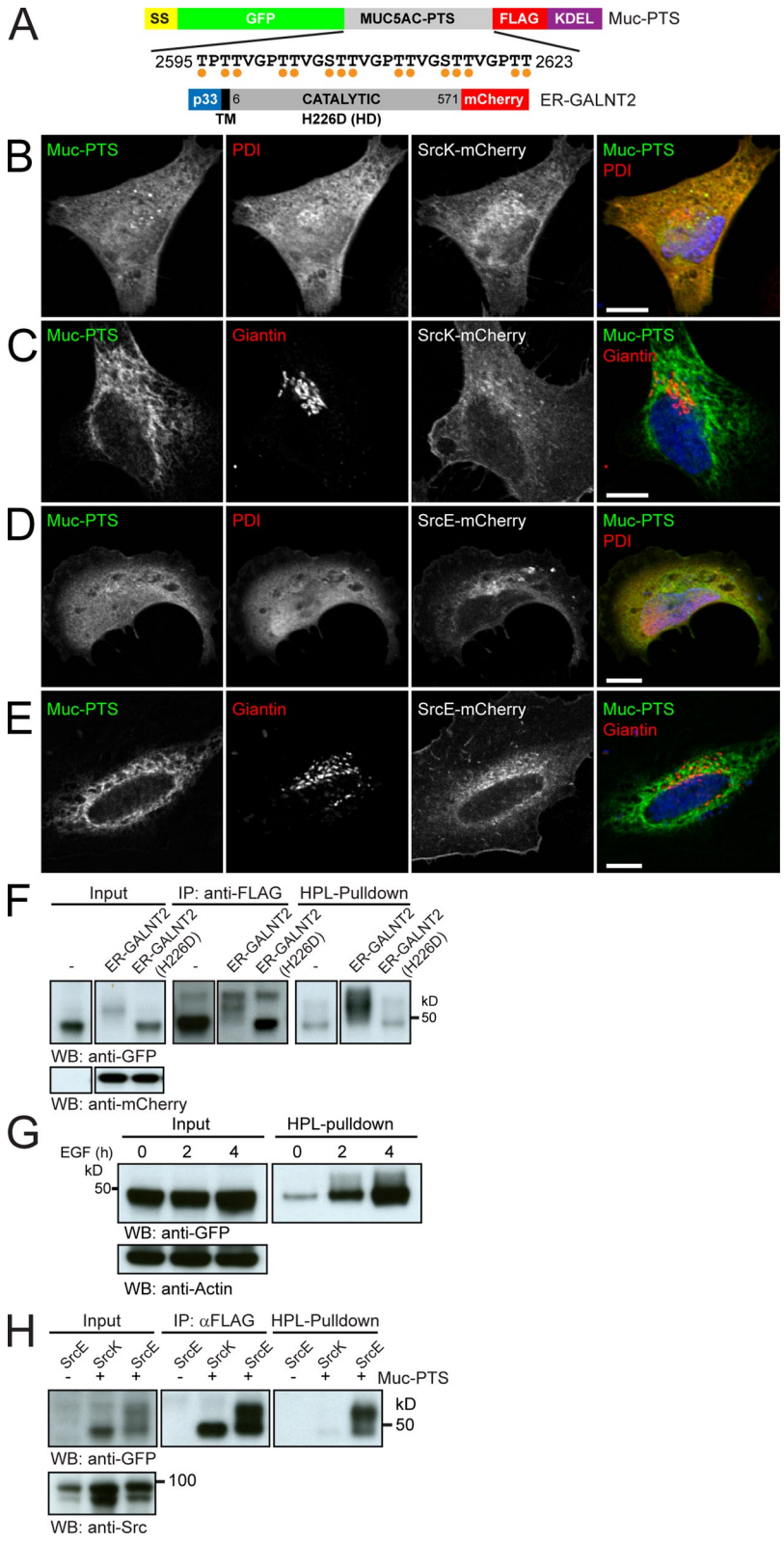

Figure 5. **An ER-trapped GalNac-T activity reporter demonstrates that GalNac-Ts are active in the ER upon Src-induced redistribution.** (A) Schematic of Muc-PTS GalNac-T activity reporter. (B and C) Immunofluorescence studies of Muc-PTS cotransfected in HeLa cells with inactive Src (SrcK-mCherry, containing K295M mutation) and staining with ER (PDI) (B) or Golgi (Giantin) (C) markers. (D and E) Immunofluorescence studies of Muc-PTS cotransfected in HeLa cells with active Src (SrcE-mCherry, containing E378G mutation) and staining with ER (D) or Golgi (E) markers. (F) SDS-PAGE analysis of Muc-PTS expressed alone in HEK293T cells or cotransfected with active (ER-GALNT2) or inactive (ER-GALNT2(H226D)) ER-targeted GalNac-T2. Muc-PTS was either immunoprecipitated with an anti-FLAG antibody or pulled down using HPL-conjugated agarose. (G) SDS-PAGE analysis of Muc-PTS pulled down using HPL-conjugated agarose after expression in HEK293T cells and treatment with EGF (100 ng/ml) for indicated times. (H) SDS-PAGE analysis of Muc-PTS coexpressed in HEK293T cells with either inactive Src (SrcK) or active SrcE (SrcE). Muc-PTS was either immunoprecipitated with an anti-FLAG antibody or pulled down using HPL-conjugated agarose. In all images nuclei were stained using Hoechst and colored blue. Bar, 10 µm.

upon GalNac-T relocation to the ER. *O*-glycosylation is known to often occur on clusters of multiple Ser or Thr residues (Fukuda and Tsuboi, 1999; Hanisch and Müller, 2000; Tarp and Clausen, 2008). For example, the prototypical MUC1 protein contains a variable number of 20 amino acid tandem repeat sequences that each contain 5 putative sites for GalNAc addition (Hanisch and Müller, 2000). To test whether the density of GalNAc modification in such a typical *O*-glycosylation cluster could be increased by GalNac-T relocation, we used a secreted reporter derived from Muc1, the Muc1-TR6 reporter (Fig. 8 E). This construct was previously reported by Müller and Hanisch (2002), with the difference that a Myc tag present in the original construct has been

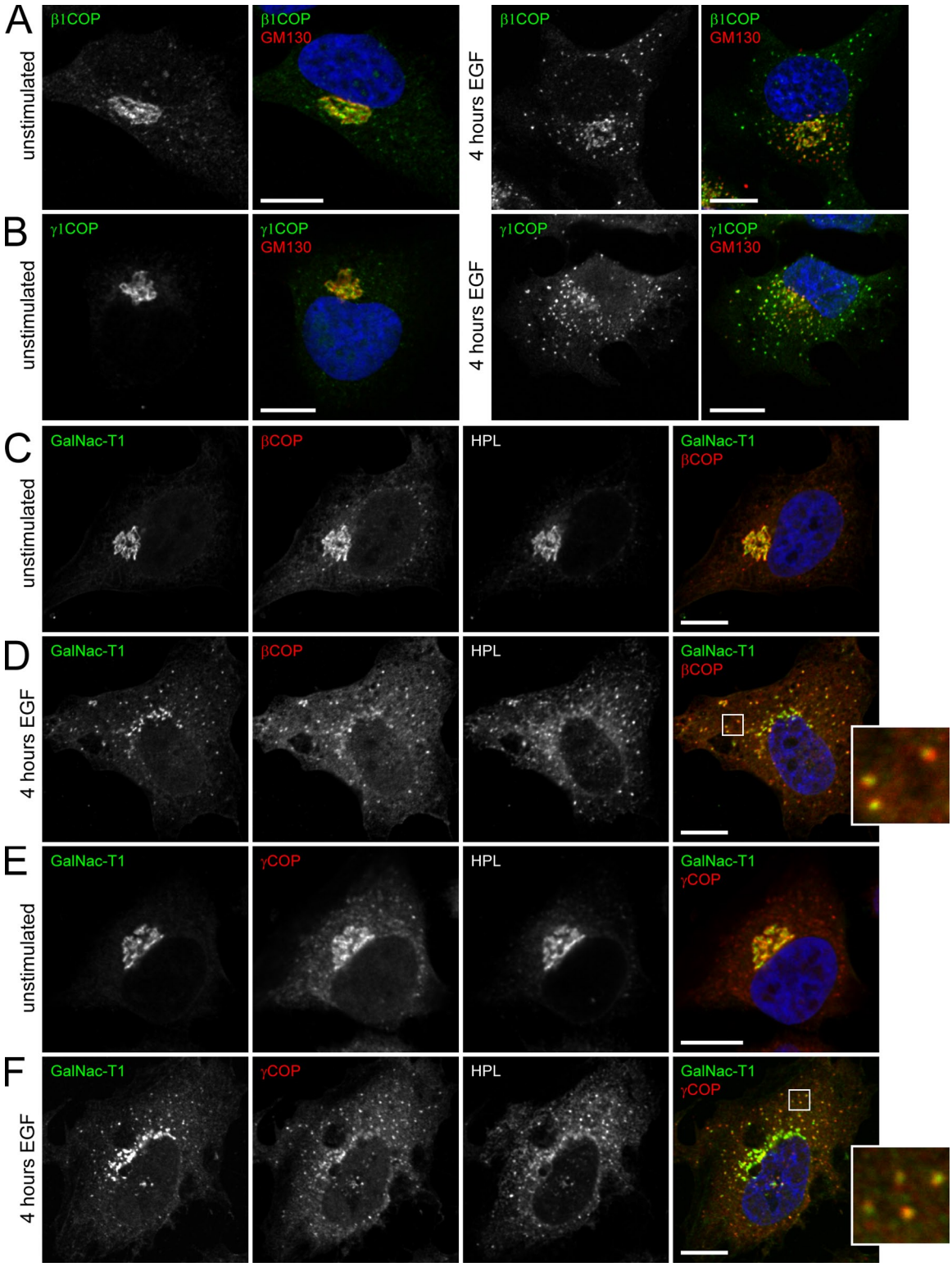

Figure 6. **Upon EGF stimulation, COP-I β1 and γ1 subunits are redistributed from the Golgi into punctate structures that also contain GalNac-T1.** (A and B) COP-I β1 (A) and γ1 (B) staining at the Golgi (Giantin) in unstimulated HeLa cells (left panels) become redistributed out of the Golgi after EGF treatment (100 ng/ml) for 4 h (right panels). The increase in number and intensity of punctate cytoplasmic COP-I–stained structures suggests that the rate of COP-I trafficking is significantly increased. (C–F) GalNac-T1 staining colocalizes with the β1 (C) or γ1 (E) COP-I subunit exclusively at the Golgi (HPL) in unstimulated HeLa cells, but also in dispersed punctate structures that stain positive for β1 (D) or γ1 (F) COP-I after EGF treatment for 4 h. In all images nuclei were stained using Hoechst and colored blue. Bar, 10 μm.

replaced here with a V5 tag. The reporter contains six Muc1 tandem repeats each with five putative sites for GalNAc addition and was found to display glycosylation densities similar to endogenous Muc1 (Müller and Hanisch, 2002). The Muc1-TR6 reporter was cotransfected with either active Src (SrcY, containing the activating point mutation Y527F) or inactive Src (SrcK)

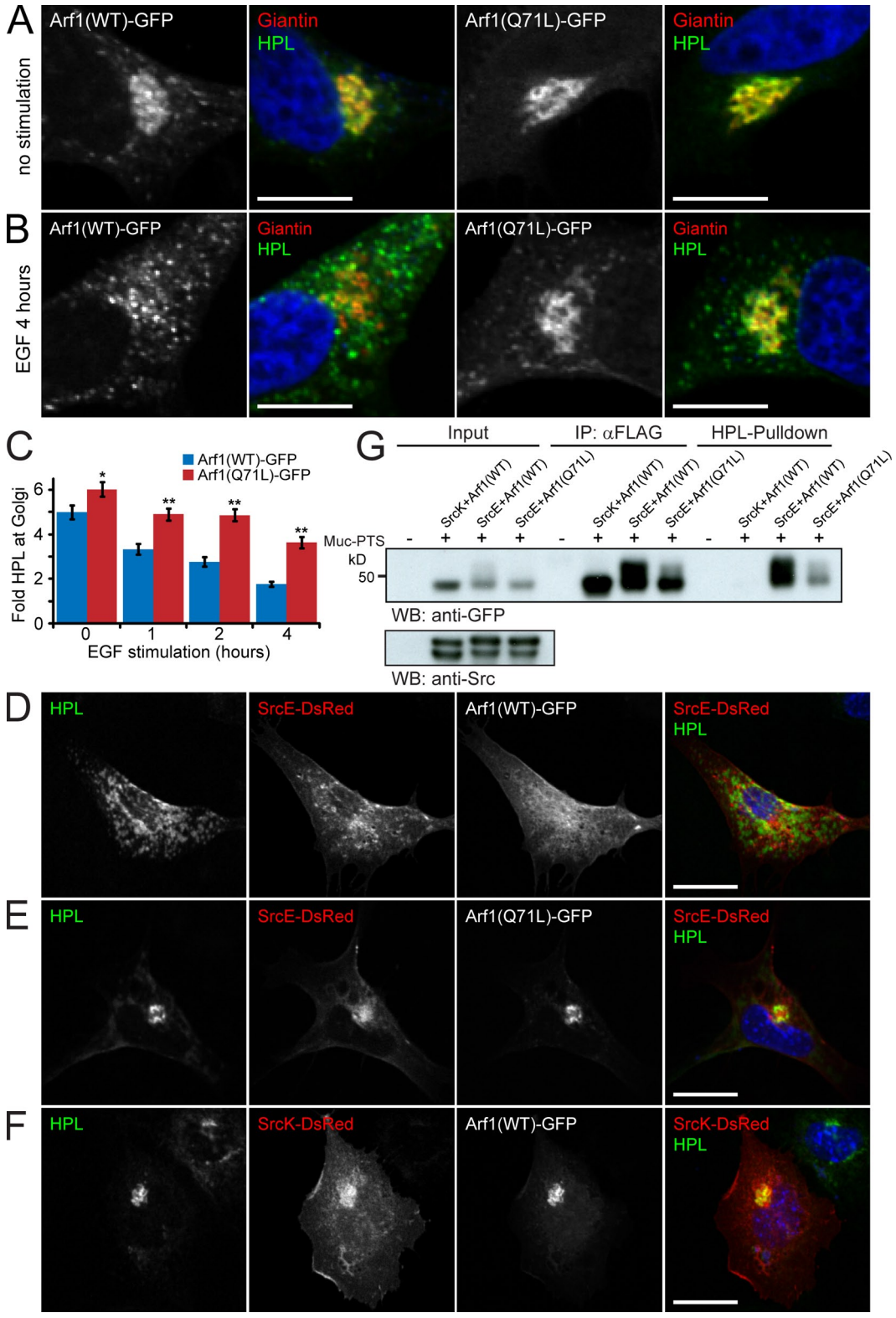

Figure 7. **A dominant-negative Arf(Q71L) mutant prevents redistribution of GalNac-Ts induced by Src activation.** (A) Wild-type Arf1-GFP (Arf1(WT)-GFP) and mutant Arf1(Q71L)-GFP colocalize primarily at the Golgi (Giantin) in unstimulated HeLa cells. (B) Expression of mutant Arf1(Q71L)-GFP (right panels) but not Arf1(WT)-GFP (left panels) resists redistribution of GalNac-Ts (indicated by HPL staining) from the Golgi to the ER under EGF treatment (100 ng/ml) for 4 h. The amount of Arf1(WT)-GFP (left panels) but not Arf1(Q71L)-GFP (right panels) at the Golgi is significantly decreased after EGF stimulation. (C) Quantification of HPL enrichment at the Golgi in HeLa cells expressing either Arf1(WT)-GFP or mutant Arf1(Q71L)-GFP after EGF treatment for indicated times. 30 cells were quantified for each sample. Error bars show SEM. Statistical significance (p) measured by two-tailed *t* test. * and **, $P < 0.05$ or $P < 0.001$, respectively, relative to mean HPL staining in cells expressing Arf1(WT)-GFP at each time point. This is a representative example from two independent experiments. (D and E) Expression of mutant Arf1(Q71L)-GFP (D) but not Arf1(WT)-GFP (E) blocks redistribution of GalNac-Ts (indicated by HPL staining) under cotransfection with active Src (SrcE-DsRed) in Src-deficient SYF fibroblasts. Active Src is enriched at the Golgi only upon expression of Arf1(Q71L)-GFP

in HEK293T cells before harvesting of the culture medium, purification of Muc1-TR6 using either Ni-NTA (binds His_6 tag) or HPL-conjugated agarose before GalNAz labeling with the Flag tag. Muc1-TR6 coexpressed with active Src contains a significantly higher density of GalNAc as judged by increased anti-FLAG staining for a similar amount of Muc1-TR6 relative to coexpression with inactive Src (Fig. 8 F). Therefore, these results indicate that Src activation can increase the density of GalNAc addition on secreted *O*-glycosylated proteins, presumably through redistribution of GalNac-Ts to the ER.

Discussion

Growth factor–induced Src signaling at the Golgi

Growth factor receptor engagement induces a vast array of responses that are often mediated by a cascade of kinase activation. In recent years it has emerged that the Golgi apparatus is regulated by kinases both during mitosis (for review see Colanzi and Corda, 2007) and interphase, for example by PKD (Van Lint et al., 2002), YSK1 (Preisinger et al., 2004), ERK (Bisel et al., 2008), and others (Preisinger and Barr, 2005). The signaling cascade consisting of heterotrimeric G protein subunits β-gamma (Jamora et al., 1999), PKD (Liljedahl et al., 2001; Bossard et al., 2007) and PKCeta (Díaz Añel and Malhotra, 2005) function to regulate TGN-to-plasma membrane traffic (Bard and Malhotra, 2006). YSK1 and ERK are proposed to regulate Golgi reorientation during cell migration through phosphorylation of GM130 and GRASP65, respectively (Preisinger et al., 2004; Bisel et al., 2008). Signaling initiated at the plasma membrane has been shown to be relayed to the Golgi apparatus, notably for small GTPases H-Ras and N-Ras (Quatela and Philips, 2006; Fehrenbacher et al., 2009). In these studies and others, activated Src was reported to be present on Golgi membranes (Bard et al., 2002; Chiu et al., 2002). The mechanisms underlying signal translocation from the plasma membrane to the Golgi remain unclear. Activated Ras appears to translocate to the Golgi by cytosolic diffusion (Goodwin et al., 2005). For Src, it is possible that membrane-anchored signaling complexes traffic from the endosomes to the Golgi (Roskoski, 2004). In addition to growth factor stimulation, Src can be activated through mutations (v-Src) or higher expression levels (SYFsrc cell line and multiple human cancers and derived cell lines; Ottenhoff-Kalff et al., 1992). Our results show that Src activation by growth factor stimulation or increased expression affects GalNac-T intracellular distribution in a similar way. Recently, it was reported that Src could be activated at the Golgi level by an increase in cargo load through the KDEL-R (Pulvirenti et al., 2008). It will be interesting to test in the future whether this mode of activation affects GalNac-T localization.

Src activation at the Golgi induces GalNac-T redistribution to the ER

GalNac-T redistribution to the ER is clear from HPL or anti-Tn antibody staining studies and from use of the ER glycosylation reporter. GalNac-Ts also localize in vesicular structures that costain with ERGIC-53 and HPL. This suggests under conditions of high Src activity, GalNac-Ts continuously cycle between the ER and the Golgi while their efficient recycling to the ER results in a shift in steady-state distribution. Src could also affect the intra-Golgi distribution of GalNac-Ts, which were shown to be present in several cisternae in HeLa cells (Röttger et al., 1998). But our current microscopic resolution is not sufficient to assess this. The ER redistribution occured with all the members of the GalNac-T family tested. By comparison, Golgi peripheral proteins (Giantin) and glycosylation enzymes (Mannosidase II and β 1,4-galactosyltransferase) are not redistributed after Src activation, suggesting that GalNac-Ts contain a feature enabling specific sorting. As the cytosolic tails of GalNac-Ts do not contain conserved tyrosines, direct phosphorylation by Src is excluded. How the GalNac-Ts are specifically sorted is therefore a particularly exciting challenge for the future.

Src mediates GalNac-T redistribution to the ER by COP-I vesicles

EGF stimulation and Src activation affect the intracellular distribution of the small GTPase Arf1 and the COP-I coat, both reducing their levels at the Golgi and generating punctate cytoplasmic structures. Some of these structures stain positive for GalNac-Ts, suggesting that GalNac-Ts are trafficked by COP-I–coated intermediates. Consistently, a dominant-negative form of Arf1, Arf1(Q71L), blocks redistribution of GalNac-Ts from the Golgi to the ER under conditions of Src activation. Interestingly, under Arf1(Q71L) expression, active Src is readily detected at the Golgi, which is usually difficult to visualize. By comparison, inactive Src accumulates readily at the Golgi (Fig. 7, E and F). A possible interpretation is that membrane-bound Src is incorporated in the GalNac-T transport intermediates that it induces. This would explain why active Src is not easily detected at the Golgi. Src vesicular trafficking will be interesting to explore in the future. Interestingly, our data suggest that COP-I–coated structures formed upon Src activation are enriched in GalNac-Ts but not other glycosyltransferases. Instances of COP-I vesicles with specific content have been previously reported (Lanoix et al., 2001; Malsam et al., 2005). Our results point to a way to induce and control the formation of a subset of COP-I vesicles, which may greatly facilitate investigation of the mechanistic basis of COP-I cargo specificity.

(E) and not Arf1(WT)-GFP (D). (F) Co-expression of Arf1(WT)-GFP and inactive Src (SrcK-DsRed) in Src-deficient SYF fibroblasts does not induce trafficking of GalNac-Ts from the Golgi (indicated by normal HPL staining). In addition, inactive Src is highly enriched at the Golgi. (G) SDS-PAGE analysis of ER-trapped Muc-PTS GalNac-T activity reporter coexpressed in HEK293T cells with either inactive Src (SrcK) or active Src (SrcE) and Arf1(WT) or Arf1(Q71L). Muc-PTS was either immunoprecipitated with an anti-FLAG antibody or pulled down using HPL-conjugated agarose. In all images nuclei were stained using Hoechst and colored blue. Bars: (A–C) 10 µm; (D–F) 20 µm.

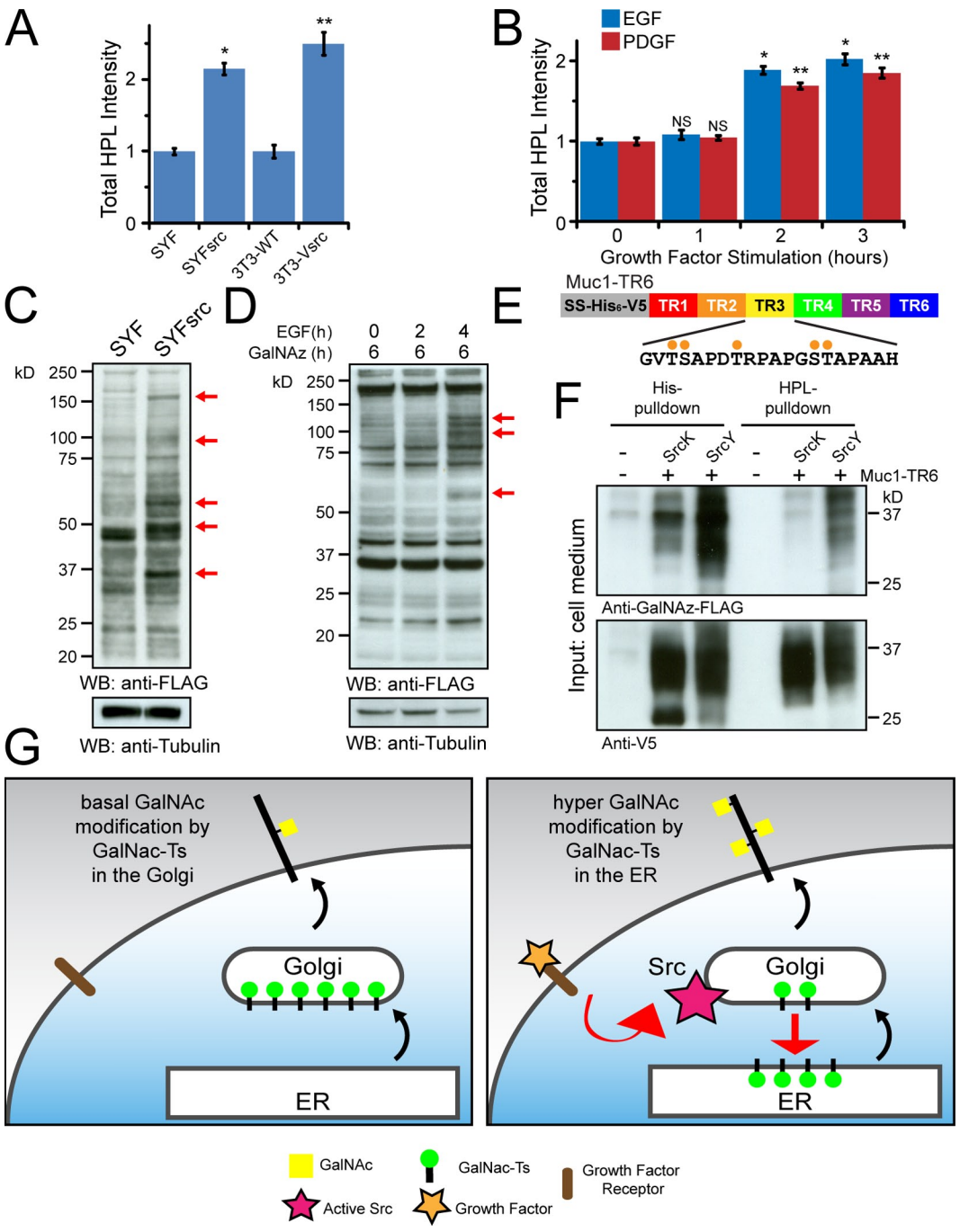

Figure 8. **Src activity increases *O*-glycosylation initiation efficiency.** (A) Quantification of total cellular HPL staining in model Src fibroblasts using a high throughput confocal microscope. At least 200 cells per well and three wells per cell line were quantified. Error bars show SEM. Statistical significance (p) was measured using a two-tailed paired *t* test. * and **, $P < 0.001$ relative to the mean HPL intensity in SYF and NIH3T3-WT cells, respectively. Normalization of SYFsrc and NIH3T3-vsrc HPL intensities was performed relative to SYF and NIH3T3-WT cell mean HPL intensities, respectively. This is a representative example from two independent experiments. (B) Quantification of total cellular HPL staining in HeLa cells treated with EGF (100 ng/ml) or PDGF (50 ng/ml) for indicated times using a high throughput confocal microscope. At least 200 cells per well and three wells per sample were quantified. Error bars show SEM. Statistical significance (p) was measured using a two-tailed paired *t* test. * and **, $P < 0.001$ relative to the mean HPL intensity in untreated cells for EGF and PDGF samples, respectively. This is a representative example from two independent experiments. (C) SDS-PAGE analysis of SYF and SYFsrc cell lysate metabolically labeled using GalNAz-FLAG. (D) SDS-PAGE analysis of unstimulated and EGF-treated HeLa cells metabolically labeled using GalNAz-FLAG for the indicated times. (E) Schematic of the Muc1-TR6 secreted *O*-glycosylation reporter. (F) SDS-PAGE analysis of secreted Muc1-TR6 purified using either agarose-conjugated Ni-NTA or HPL before labeling with GalNAz-FLAG. (G) A model for Src-induced Golgi-to-ER retrograde trafficking of GalNac-T enzymes. Under normal cellular conditions, GalNac-Ts are predominantly localized to the cis-face of the Golgi apparatus and initiation of *O*-glycosylation occurs in the Golgi apparatus. Upon activation of Src, GalNac-Ts are selectively trafficked to the ER. This increases the efficiency of *O*-glycosylation initiation and results in a greater density of GalNAc added onto mucin-like proteins (further *O*-glycan modifications are not included for sake of clarity).

Src activation up-regulates *O*-GalNAc glycosylation through GalNac-T redistribution

Constitutive high Src activity and activation of Src after growth factor stimulation results in higher total cell intensity labeling with HPL, suggesting more GalNAc is incorporated into proteins. Consistently, GalNaz metabolic labeling reveals several proteins with de novo or enhanced GalNAc incorporation, indicating that normally unmodified Ser or Thr residues are becoming *O*-glycosylated upon Src activation. This is observed at the whole-cell level and could concern ER-localized proteins. However, the secreted reporter Muc1-TR6 purified from cell supernatant also has enhanced glycosylation, indicating that the *O*-GalNAc increase affects secreted and cell surface proteins. The de novo addition of GalNAc could occur on Ser or Thr residues hidden after full protein folding but exposed in the ER. Alternatively, de novo glycosylation could also occur in "hot-spots" partially glycosylated when GalNac-Ts are restricted to the Golgi. This is clearly occurring with the Muc1-TR6 secreted reporter, which contains 30 possible sites (6 tandem repeats each with 5 possible sites). High-density glycan attachment is a hallmark of numerous *O*-GalNAc glycosylated proteins. Muc1, for example, contains a polymorphic central region of up to 120 tandem repeats, resulting in a potential number of 600 *O*-glycans per central region (Hanisch and Müller, 2000). The density of *O*-glycan chains on Muc1 tandem repeats is variable. For example, Muc1 from lactating breast or from cancer cell lines contains an average of 2.6 and 4.8 glycans per repeat, respectively (Müller et al., 1997, 1999; Müller and Hanisch, 2002). *O*-glycan density can also vary depending on cell activation status (Wu et al., 2009).

These variations have usually been attributed to changes in glycosyltransferase expression patterns, but our study suggests that intracellular distribution could be an important factor. How exactly redistribution favors higher density is not clear at this stage. It might simply allow more time for the GalNac-Ts to modify their protein substrates. Alternatively, redistribution of GalNac-Ts to an earlier compartment could lower their competition with other enzymes. Indeed, GalNac-Ts are sensitive to neighboring site glycosylation status (Gerken et al., 2002, 2004) and require their lectin domain for high density *O*-GalNAc glycosylation (Wandall et al., 2007). The lectin domain binds α-linked GalNAc residues and will therefore be affected by the core forming enzymes which modify the GalNac residue.

Potential physiological significance of *O*-GalNAc glycosylation regulation

O-GalNAc glycans have been implicated in multiple and diverse physiological functions (for reviews see Hang and Bertozzi, 2005; Brockhausen, 2006; Tarp and Clausen, 2008; Tian and Ten Hagen, 2009). Consistently, the extent and specific types of *O*-glycans are known to vary extensively between tissues (Brockhausen, 2006) and during development (Laughlin et al., 2008; Laughlin and Bertozzi, 2009). Recently, genetic deletions in mice and *Drosophila* have revealed essential roles for GalNac-Ts and enzymes acting downstream (Tian and Ten Hagen, 2009). Redistribution of GalNac-Ts to the ER could affect cell physiology in multiple ways, for example, by altering ER resident proteins. It could affect the folding and activity of secreted proteins or affect their sensitivity to proteases. Indeed, glycosylation often protects glycoproteins from proteolytic degradation. For example, *O*-GalNAc glycosylation competes with trans-Golgi proprotein convertase cleavage of the FGF23 secreted factor (Kato et al., 2006). One interesting possibility is that the increase in *O*-glycan chain density could affect the type of *O*-glycans synthesized. Recently, high-density GalNAc modification was shown to inhibit the core forming enzymes that extend the glycan chain (Brockhausen et al., 2009). GalNac-T relocation induced by Src could therefore favor shorter glycan chain lengths. Interestingly, it has long been observed that cancerous transformation is often associated with an increase in short *O*-glycans such as the Tn, sialylated Tn, and T antigens (Brockhausen, 2006). These changes in glycans types could in turn affect binding of lectin molecules. *O*-glycan–specific lectins such as the selectins have indeed been shown to be essential for lymphocyte adhesion (Tian and Ten Hagen, 2009). Regulation of cell adhesion by *O*-glycans has been shown in vitro for cancer cell lines (Clément et al., 2004; Julien et al., 2005, 2006) and genetically in the *Drosophila* wing where deletion of pgant3, a GalNac-T, leads to loss of adhesion between epithelial sheets and blisters (Zhang et al., 2008). Perturbation of cell adhesion could facilitate cell migration and metastasis in vivo, perhaps explaining the poor prognosis of cancer patients found to have short *O*-glycans (Itzkowitz et al., 1990; Nakamori et al., 1993; Ogata et al., 1998). Interestingly, Src regulates both cell adhesion and cell migration and has been associated with metastasis in vivo (Yeatman, 2004). Therefore, it is tempting to speculate that regulation of *O*-glycosylation by GalNac-T redistribution plays a significant role in Src-mediated regulation of cell adhesion and migration in vitro and metastasis in vivo.

Materials and methods

Cloning

Plasmids encoding full-length wild-type chicken SRC and an E378G-containing point mutant were a gift from Roland Baron (Harvard Medical School, Boston, MA). A plasmid encoding full-length HA-tagged Mannosidase I-C was a gift from Annette Hercovics (McGill Cancer Center, Montreal, Canada). A plasmid encoding full-length C2GnT was a gift from Minoru Fukuda (Burnham Institute, San Diego, CA). Full-length SRC was amplified by PCR using attB-containing primers and cloned into pDONR221 using BP-clonase II (Invitrogen). Human GALNT2 (GenBank/EMBL/DDBJ accession no. NM_004481), ARF1 (NM_001024227), and a short sequence (7746–8033) from the human MUC5AC gene (XM_001130382) were PCR amplified and cloned into pDONR221 from cDNA synthesized using SuperScript-III (Invitrogen) and total RNA extracted from HT29-18N_2 cells. Addition of the FLAG(DYKDDDDK)-KDEL sequence to the Muc5AC entry clone was achieved by PCR using a primer extension method before reamplification using attB-containing primers and cloning into pDONR221. Replacement of the N terminus (residues 1–5) of GALNT2 with the N terminus (residues 1–46) of MHC class II light chain invariant protein p33 (NM_001025159) was achieved by PCR using attB-containing primers before cloning into pDONR221. The Muc1-TR6 *O*-glycosylation reporter was constructed by PCR before reamplification using attB-containing primers and cloning into pDONR221. All point mutants were introduced into GALNT2-, ARF1-, and SRC-containing pDONR221 entry clones by PCR using overlapping mutagenic primers and KOD polymerase (Merck). Human Muc5AC-PTS-KDEL was subcloned into pFB-ssHGH-NemGFP-DEST (N-terminal ER signal sequence from human growth hormone fused to emGFP). SRC and GALNT2 were subcloned into pFB-CDsRed-DEST and pFB-CmCherry-DEST (C-terminal DsRed or mCherry tags). C2GnT was subcloned into pDsRed-Monomer-Hyg-N1 (Takara Bio Inc.) using NheI/BamHI

restriction enzymes (C-terminal DsRed tag). ARF1 was subcloned into pFB-CemGFP-DEST (C-terminal emGFP tag) and pcDNA-DEST40 (C-terminal V5-His_6 tag) (Invitrogen). Muc1-TR6 was subcloned into pcDNA-DEST40 (no C-terminal tag added due to presence of a stop codon in the Muc1 sequence). The pAcGFP-Golgi plasmid encoding residues 1–81 of human β 1,4-galactosyltransferase (GalT) fused at its C terminus to GFP was also used (Takara Bio Inc.). All constructs were verified by sequencing before use.

Cell culture

SYF and SYFsrc mouse fibroblast cell lines were a gift from V. Malhotra (Centre for Genomic Regulation, Barcelona, Spain). WI38 human fibroblast cells, HEK293T cells, and NIH3T3 and NIH3T3-vsrc mouse fibroblast cells were a gift from W. Hong, V. Tergaonkar, and X. Cao, respectively (IMCB, Singapore). All cells were grown at 37°C in a 10% CO_2 incubator. SYF, SYFsrc, NIH3T3, and NIH3T3-vsrc cells were grown in DME supplemented with 10% fetal bovine serum (FBS). HEK293T cells were grown in DME supplemented with 15% FBS. WI38 cells were grown in MEM supplemented with 10% FBS.

Immunofluorescence microscopy

Cells were seeded at desired densities onto glass coverslips in 24-well dishes (Thermo Fisher Scientific). After incubation at 37°C and 10% CO_2 for 8–16 h, cells were transfected using FugeneHD (Roche) as per manufacturer's instructions. For growth factor stimulation experiments, cells were washed once using Dulbecco's phosphate-buffered saline (D-PBS) before overnight serum starvation in DME (no FBS). Human recombinant EGF (100 ng/ml; Sigma-Aldrich) or mouse recombinant PDGF-bb (50 ng/ml; Invitrogen) was added along with either DMSO (no inhibitor) or 10 µM Src Inhibitor (SU6656 or Src kinase inhibitor I; Merck). Metabolic labeling of SYF and SYFsrc cells with 50 µM GalNAz (Sigma-Aldrich) was performed overnight in DME supplemented with 10% FBS. Metabolic labeling of serum-starved HeLa cells with 50 µM GalNAz was performed for up to 6 h in DME after serum starvation overnight. All subsequent steps were performed at room temperature. Cells were washed for 10 min with D-PBS, fixed for 10 min using 4% paraformaldehyde in D-PBS, washed for a further 10 min with D-PBS, and permeabilized with 0.2% Triton X-100 in D-PBS for 5 min. Cells were blocked twice for 10 min each with 2% FBS in D-PBS before antibody staining following the manufacturer's instructions. Anti-GalNac-T1, -T2, -T3, -T4, -T6, and anti-Tn hybridomas were a gift from U. Mendel and H. Clausen (University of Copenhagen, Copenhagen, Denmark). Cells were further washed twice using 2% FBS in D-PBS and subsequently stained for 15–30 min with secondary Alexa Fluor–conjugated antibodies and Hoechst (Invitrogen). For cells stained with HPL, either Alexa 488– (Invitrogen) or 647–conjugated (Invitrogen) HPL was added during secondary antibody incubations. Cells were mounted onto glass slides using FluorSave (Merck) and imaged at room temperature using an inverted FluoView confocal microscope (model IX81; Olympus) coupled with a CCD camera (model FVII) either with a 60x objective (U Plan Super Apochromatic [UPLSAPO]; NA 1.35) or 100x objective (UPLSAPO; NA 1.40) under Immersol oil. Images were acquired and processed using Olympus FV10-ASW software.

HPL staining quantification

SYF, SYFsrc, NIH3T3, and NIH3T3-vsrc cells were seeded at 10,000 cells per well in a 96-well clear and flat-bottomed black imaging plate (BD) and incubated overnight at 37°C and 10% CO_2. Alternatively, HeLa cells were seeded into imaging plates before serum starvation and treatment with EGF or PDGF as outlined above. Cells were fixed, permeabilized, and stained with Hoechst and Alexa 647–conjugated HPL as outlined above before storage in D-PBS. Cells were imaged at room temperature using a high throughput ImageXpress^{ULTRA} confocal microscope with a 40x Plan Fluor objective (MDS Analytical Technologies). Images were processed using the Transfluor HT module of the MetaXpress analysis software (MDS Analytical Technologies). In brief, a target compartment delineated by the HPL fluorescence was acquired (using an intensity-based cutoff) before quantification of the integrated intensity of HPL staining within that compartment. Hundreds of cells were quantified and the averages as well as the SEM were calculated. Statistical significance was measured using a paired *t* test assuming a two-tailed Gaussian distribution. For high magnification confocal images (60x objective), ∼60 cells were acquired per conditions. Cells in mitosis, with out-of-focus or highly fragmented Golgi staining, were excluded and then a total of 30 cells were chosen at random for each condition. Because HPL and GalNAc-T staining are uniformly distributed in the Golgi and in cytoplasm around the Golgi, the analysis of intensities along a line randomly drawn over the Golgi apparatus and the perinuclear cytoplasm is representative of the corresponding volumes. The Golgi region and cytoplasm regions were determined using the intensity of the Golgi marker (GM130 or Giantin) staining (Fig. 1 C). The ratio of average intensity at the Golgi (along the line) over intensity average in the cytoplasm was then calculated. The ratio was averaged for 30 cells and the SEM was calculated. Statistical significance was measured using a paired *t* test assuming a two-tailed Gaussian distribution.

***O*-glycosylation reporter analysis**

HEK293T cells were transfected using a calcium phosphate method. In brief, 1-ml transfection complexes composed of 10–30 µg of DNA diluted in 250 mM calcium phosphate and mixed with BBS buffer (140 mM sodium chloride, 0.7 mM disodium hydrogen phosphate, and 25 mM *N,N*-Bis(2-hydroxyethyl)-2-aminoethanesulfonic acid [BES], pH 6.95 [20°C]) by vortex were incubated at room temperature for 15 min before addition to cells. HEK293T cells were seeded 8–24 h before addition of transfection complex to obtain an optimal confluency (80–90%) for transfection. The next day, the growth medium was replaced and the cells were further incubated for 24–48 h. Metabolic labeling of HEK293T cells with 20 µM GalNAz was performed 24 h before transfection with Muc1(TR6) *O*-glycosylation reporter. Cells were further incubated for 30 h before replacement of the medium with low serum opti-MEM (Invitrogen), which was harvested after an additional 24 h. Cells were washed twice using ice-cold D-PBS before scraping in D-PBS. Cells were centrifuged at 300 *g* for 5 min at 4°C and the cell pellet snap-frozen in liquid N_2. All cell pellets were stored at −80°C until use. Cells were thawed on ice in the presence of ice-cold immunoprecipitation (IP) lysis buffer (50 mM Tris [pH 8.0, 4°C], 200 mM NaCl, 0.5% NP-40 alternative, 1 mM DTT, and complete protease inhibitor [Roche]) for 30 min with gradual agitation before clarification of samples by centrifugation at 10,000 *g* for 10 min at 4°C. DTT was omitted in all GalNAz labeling experiments. Clarified lysate protein concentrations were determined using Bradford reagent (Bio-Rad Laboratories) before sample normalization. All subsequent steps were performed either on ice or at 4°C. IP samples were incubated with 1–2 µg of IP antibody or HPL-conjugated agarose (Sigma-Aldrich) overnight at 4°C. The next day, antibody-containing lysates were incubated with 20 µl of washed protein G–Sepharose. IP samples were washed a total of 5 times using 1 ml of IP wash buffer (50 mM Tris [pH 8.0, 4°C], 100 mM NaCl, 0.5% NP-40 alternative, 1 mM DTT, and complete protease inhibitor [Roche]). DTT was omitted in all GalNAz labeling IP experiments. Samples were diluted in IP wash buffer to a final volume of 45 µl (including resin) before addition of 15 µl 4x SDS loading buffer and boiling at 95°C for 2 min. Samples were resolved by SDS-PAGE electrophoresis using bis-tris NuPage gels as per manufacturer's instructions (Invitrogen). Samples were transferred to PVDF membranes and blocked using 3% BSA dissolved in TBST (50 mM Tris [pH 8.0, 4°C], 150 mM NaCl, and 0.1% Tween 20) for 2 h at room temperature or overnight at 4°C. Membranes were washed to remove traces of BSA before incubation with antibodies as per manufacturer's instructions. Membranes were washed five times with TBST before incubation with secondary HRP-conjugated antibodies (GE Healthcare). Membranes were further washed five times with TBST before ECL exposure.

Microinjection

SYF and WI38 cells were seeded at desired densities in 35-mm glass-bottom Petri dishes (MatTek) and incubated overnight at 37°C and 10% CO_2. The next day, media was supplemented with 20 mM Hepes (pH 7.0; 20°C) before cells were microinjected using a 0.5-µm Femtotip-loaded microinjector (model 5242; Eppendorf) equipped with a microscope (Axiovert 35; Carl Zeiss, Inc.) fitted with a heated stage. DNA constructs were diluted to 25 ng/µl and centrifuged for 10 min at 10,000 *g* before microinjection into the cell nuclei at 90 hPa for 0.4 s. For co-microinjection, DNA constructs were mixed in a 1:1 molar ratio to yield a final concentration of 25 ng/µl. Cells were incubated at 37°C and 10% CO_2 for indicated times before either live cell imaging or fixation and staining as outlined above.

Online supplemental material

Fig. S1 shows HPL, Tn, and GalNac-T1 intracellular staining being redistributed away from the Golgi in HeLa cells treated with PDGF. Fig. S2 illustrates that inhibition of transcription using α-Amanitin in HeLa cells during EGF stimulation does not affect HPL redistribution. Fig. S3 highlights that intracellular HPL staining is redistributed away from the Golgi upon EGF or PDGF stimulation only in Src-activated SYFsrc fibroblasts and not Src-deficient SYF fibroblasts. Fig. S4 shows that endogenous GalNac-T1, -T4, and -T6 enzymes are redistributed away from the Golgi in WI38 human fibroblasts microinjected with a Src expression plasmid. Fig. S5 demonstrates that ManIC, C2GnT, and GalT glycosyltransferases as well as GM130 protein are not redistributed from the Golgi under increased

Src activity. Online supplemental material is available at http://www.jcb.org/cgi/content/full/jcb.201003055/DC1.

We thank Ivan Tan and Hsiangling Teo for assistance with microinjection and HEK293T transfection experiments, respectively.

The Bard laboratory is supported by A*Star funds. D.J. Gill is also supported by an EMBO long-term fellowship.

Submitted: 12 March 2010
Accepted: 27 April 2010

References

Bard, F., and V. Malhotra. 2006. The formation of TGN-to-plasma-membrane transport carriers. *Annu. Rev. Cell Dev. Biol.* 22:439–455. doi:10.1146/annurev.cellbio.21.012704.133126

Bard, F., U. Patel, J.B. Levy, P. Jurdic, W.C. Horne, and R. Baron. 2002. Molecular complexes that contain both c-Cbl and c-Src associate with Golgi membranes. *Eur. J. Cell Biol.* 81:26–35. doi:10.1078/0171-9335-00217

Bard, F., L. Mazelin, C. Péchoux-Longin, V. Malhotra, and P. Jurdic. 2003. Src regulates Golgi structure and KDEL receptor-dependent retrograde transport to the endoplasmic reticulum. *J. Biol. Chem.* 278:46601–46606. doi:10.1074/jbc.M302221200

Bisel, B., Y. Wang, J.H. Wei, Y. Xiang, D. Tang, M. Miron-Mendoza, S. Yoshimura, N. Nakamura, and J. Seemann. 2008. ERK regulates Golgi and centrosome orientation towards the leading edge through GRASP65. *J. Cell Biol.* 182:837–843. doi:10.1083/jcb.200805045

Bossard, C., D. Bresson, R.S. Polishchuk, and V. Malhotra. 2007. Dimeric PKD regulates membrane fission to form transport carriers at the TGN. *J. Cell Biol.* 179:1123–1131. doi:10.1083/jcb.200703166

Brockhausen, I. 2006. Mucin-type O-glycans in human colon and breast cancer: glycodynamics and functions. *EMBO Rep.* 7:599–604. doi:10.1038/sj.embor.7400705

Brockhausen, I., T. Dowler, and H. Paulsen. 2009. Site directed processing: role of amino acid sequences and glycosylation of acceptor glycopeptides in the assembly of extended mucin type O-glycan core 2. *Biochim. Biophys. Acta.* 1790:1244–1257.

Chiu, V.K., T. Bivona, A. Hach, J.B. Sajous, J. Silletti, H. Wiener, R.L. Johnson II, A.D. Cox, and M.R. Philips. 2002. Ras signalling on the endoplasmic reticulum and the Golgi. *Nat. Cell Biol.* 4:343–350.

Clément, M., J. Rocher, G. Loirand, and J. Le Pendu. 2004. Expression of sialyl-Tn epitopes on beta1 integrin alters epithelial cell phenotype, proliferation and haptotaxis. *J. Cell Sci.* 117:5059–5069. doi:10.1242/jcs.01350

Colanzi, A., and D. Corda. 2007. Mitosis controls the Golgi and the Golgi controls mitosis. *Curr. Opin. Cell Biol.* 19:386–393. doi:10.1016/j.ceb.2007.06.002

Crocker, P.R., and P. Redelinghuys. 2008. Siglecs as positive and negative regulators of the immune system. *Biochem. Soc. Trans.* 36:1467–1471. doi:10.1042/BST0361467

D'Souza-Schorey, C., and P. Chavrier. 2006. ARF proteins: roles in membrane traffic and beyond. *Nat. Rev. Mol. Cell Biol.* 7:347–358. doi:10.1038/nrm1910

Dascher, C., and W.E. Balch. 1994. Dominant inhibitory mutants of ARF1 block endoplasmic reticulum to Golgi transport and trigger disassembly of the Golgi apparatus. *J. Biol. Chem.* 269:1437–1448.

David-Pfeuty, T., and Y. Nouvian-Dooghe. 1990. Immunolocalization of the cellular src protein in interphase and mitotic NIH c-src overexpresser cells. *J. Cell Biol.* 111:3097–3116. doi:10.1083/jcb.111.6.3097

Díaz Añel, A.M., and V. Malhotra. 2005. PKCeta is required for beta-1gamma2/beta3gamma2- and PKD-mediated transport to the cell surface and the organization of the Golgi apparatus. *J. Cell Biol.* 169:83–91. doi:10.1083/jcb.200412089

Fehrenbacher, N., D. Bar-Sagi, and M. Philips. 2009. Ras/MAPK signaling from endomembranes. *Mol. Oncol.* 3:297–307. doi:10.1016/j.molonc.2009.06.004

Freeze, H.H. 2006. Genetic defects in the human glycome. *Nat. Rev. Genet.* 7:537–551. doi:10.1038/nrg1894

Fritz, T.A., J.H. Hurley, L.B. Trinh, J. Shiloach, and L.A. Tabak. 2004. The beginnings of mucin biosynthesis: the crystal structure of UDP-GalNAc:polypeptide alpha-N-acetylgalactosaminyltransferase-T1. *Proc. Natl. Acad. Sci. USA.* 101:15307–15312. doi:10.1073/pnas.0405657101

Fukuda, M., and S. Tsuboi. 1999. Mucin-type O-glycans and leukosialin. *Biochim. Biophys. Acta.* 1455:205–217.

Gerken, T.A., J. Zhang, J. Levine, and A. Elhammer. 2002. Mucin core O-glycosylation is modulated by neighboring residue glycosylation status. Kinetic modeling of the site-specific glycosylation of the apo-porcine submaxillary mucin tandem repeat by UDP-GalNAc:polypeptide N-acetylgalactosaminyltransferases T1 and T2. *J. Biol. Chem.* 277:49850–49862. doi:10.1074/jbc.M205851200

Gerken, T.A., C. Tep, and J. Rarick. 2004. Role of peptide sequence and neighboring residue glycosylation on the substrate specificity of the uridine 5′-diphosphate-alpha-N-acetylgalactosamine:polypeptide N-acetylgalactosaminyl transferases T1 and T2: kinetic modeling of the porcine and canine submaxillary gland mucin tandem repeats. *Biochemistry.* 43:9888–9900. doi:10.1021/bi049178e

Goodwin, J.S., K.R. Drake, C. Rogers, L. Wright, J. Lippincott-Schwartz, M.R. Philips, and A.K. Kenworthy. 2005. Depalmitoylated Ras traffics to and from the Golgi complex via a nonvesicular pathway. *J. Cell Biol.* 170:261–272. doi:10.1083/jcb.200502063

Hang, H.C., and C.R. Bertozzi. 2005. The chemistry and biology of mucin-type O-linked glycosylation. *Bioorg. Med. Chem.* 13:5021–5034. doi:10.1016/j.bmc.2005.04.085

Hanisch, F.G. 2001. O-glycosylation of the mucin type. *Biol. Chem.* 382:143–149. doi:10.1515/BC.2001.022

Hanisch, F.G., and S. Müller. 2000. MUC1: the polymorphic appearance of a human mucin. *Glycobiology.* 10:439–449. doi:10.1093/glycob/10.5.439

Hsu, V.W., S.Y. Lee, and J.S. Yang. 2009. The evolving understanding of COPI vesicle formation. *Nat. Rev. Mol. Cell Biol.* 10:360–364. doi:10.1038/nrm2663

Ichikawa, S., A.H. Sorenson, A.M. Austin, D.S. Mackenzie, T.A. Fritz, A. Moh, S.L. Hui, and M.J. Econs. 2009. Ablation of the Galnt3 gene leads to low-circulating intact fibroblast growth factor 23 (Fgf23) concentrations and hyperphosphatemia despite increased Fgf23 expression. *Endocrinology.* 150:2543–2550. doi:10.1210/en.2008-0877

Itzkowitz, S.H., E.J. Bloom, W.A. Kokal, G. Modin, S. Hakomori, and Y.S. Kim. 1990. Sialosyl-Tn. A novel mucin antigen associated with prognosis in colorectal cancer patients. *Cancer.* 66:1960–1966. doi:10.1002/1097-0142(19901101)66:9<1960::AID-CNCR2820660919>3.0.CO;2-X

Jamora, C., N. Yamanouye, J. Van Lint, J. Laudenslager, J.R. Vandenheede, D.J. Faulkner, and V. Malhotra. 1999. Gbetagamma-mediated regulation of Golgi organization is through the direct activation of protein kinase D. *Cell.* 98:59–68. doi:10.1016/S0092-8674(00)80606-6

Julien, S., C. Lagadec, M.A. Krzewinski-Recchi, G. Courtand, X. Le Bourhis, and P. Delannoy. 2005. Stable expression of sialyl-Tn antigen in T47-D cells induces a decrease of cell adhesion and an increase of cell migration. *Breast Cancer Res. Treat.* 90:77–84. doi:10.1007/s10549-004-3137-3

Julien, S., E. Adriaenssens, K. Ottenberg, A. Furlan, G. Courtand, A.S. Vercoutter-Edouart, F.G. Hanisch, P. Delannoy, and X. Le Bourhis. 2006. ST6GalNAc I expression in MDA-MB-231 breast cancer cells greatly modifies their O-glycosylation pattern and enhances their tumourigenicity. *Glycobiology.* 16:54–64. doi:10.1093/glycob/cwj033

Kato, K., C. Jeanneau, M.A. Tarp, A. Benet-Pagès, B. Lorenz-Depiereux, E.P. Bennett, U. Mandel, T.M. Strom, and H. Clausen. 2006. Polypeptide GalNAc-transferase T3 and familial tumoral calcinosis. Secretion of fibroblast growth factor 23 requires O-glycosylation. *J. Biol. Chem.* 281:18370–18377. doi:10.1074/jbc.M602469200

Klinghoffer, R.A., C. Sachsenmaier, J.A. Cooper, and P. Soriano. 1999. Src family kinases are required for integrin but not PDGFR signal transduction. *EMBO J.* 18:2459–2471. doi:10.1093/emboj/18.9.2459

Lanoix, J., J. Ouwendijk, A. Stark, E. Szafer, D. Cassel, K. Dejgaard, M. Weiss, and T. Nilsson. 2001. Sorting of Golgi resident proteins into different subpopulations of COPI vesicles: a role for ArfGAP1. *J. Cell Biol.* 155:1199–1212. doi:10.1083/jcb.200108017

Laughlin, S.T., and C.R. Bertozzi. 2007. Metabolic labeling of glycans with azido sugars and subsequent glycan-profiling and visualization via Staudinger ligation. *Nat. Protoc.* 2:2930–2944. doi:10.1038/nprot.2007.422

Laughlin, S.T., and C.R. Bertozzi. 2009. In vivo imaging of *Caenorhabditis elegans* glycans. *ACS Chem. Biol.* 4:1068–1072. doi:10.1021/cb900254y

Laughlin, S.T., J.M. Baskin, S.L. Amacher, and C.R. Bertozzi. 2008. In vivo imaging of membrane-associated glycans in developing zebrafish. *Science.* 320:664–667. doi:10.1126/science.1155106

Ley, K., and G.S. Kansas. 2004. Selectins in T-cell recruitment to non-lymphoid tissues and sites of inflammation. *Nat. Rev. Immunol.* 4:325–335. doi:10.1038/nri1351

Liljedahl, M., Y. Maeda, A. Colanzi, I. Ayala, J. Van Lint, and V. Malhotra. 2001. Protein kinase D regulates the fission of cell surface destined transport carriers from the trans-Golgi network. *Cell.* 104:409–420. doi:10.1016/S0092-8674(01)00228-8

Malsam, J., A. Satoh, L. Pelletier, and G. Warren. 2005. Golgin tethers define subpopulations of COPI vesicles. *Science.* 307:1095–1098. doi:10.1126/science.1108061

Müller, S., and F.G. Hanisch. 2002. Recombinant MUC1 probe authentically reflects cell-specific O-glycosylation profiles of endogenous breast cancer mucin. High density and prevalent core 2-based glycosylation. *J. Biol. Chem.* 277:26103–26112. doi:10.1074/jbc.M202921200

Müller, S., S. Goletz, N. Packer, A. Gooley, A.M. Lawson, and F.G. Hanisch. 1997. Localization of O-glycosylation sites on glycopeptide fragments from lactation-associated MUC1. All putative sites within the tandem repeat are glycosylation targets in vivo. *J. Biol. Chem.* 272:24780–24793. doi:10.1074/jbc.272.40.24780

Müller, S., K. Alving, J. Peter-Katalinic, N. Zachara, A.A. Gooley, and F.G. Hanisch. 1999. High density O-glycosylation on tandem repeat peptide from secretory MUC1 of T47D breast cancer cells. *J. Biol. Chem.* 274:18165–18172. doi:10.1074/jbc.274.26.18165

Nakamori, S., M. Kameyama, S. Imaoka, H. Furukawa, O. Ishikawa, Y. Sasaki, T. Kabuto, T. Iwanaga, Y. Matsushita, and T. Irimura. 1993. Increased expression of sialyl Lewisx antigen correlates with poor survival in patients with colorectal carcinoma: clinicopathological and immunohistochemical study. *Cancer Res.* 53:3632–3637.

Ogata, S., R. Koganty, M. Reddish, B.M. Longenecker, A. Chen, C. Perez, and S.H. Itzkowitz. 1998. Different modes of sialyl-Tn expression during malignant transformation of human colonic mucosa. *Glycoconj. J.* 15:29–35. doi:10.1023/A:1006935331756

Ottenhoff-Kalff, A.E., G. Rijksen, E.A. van Beurden, A. Hennipman, A.A. Michels, and G.E. Staal. 1992. Characterization of protein tyrosine kinases from human breast cancer: involvement of the c-src oncogene product. *Cancer Res.* 52:4773–4778.

Pathak, R.K., R.K. Merkle, R.D. Cummings, J.L. Goldstein, M.S. Brown, and R.G. Anderson. 1988. Immunocytochemical localization of mutant low density lipoprotein receptors that fail to reach the Golgi complex. *J. Cell Biol.* 106:1831–1841. doi:10.1083/jcb.106.6.1831

Perez-Vilar, J., J. Hidalgo, and A. Velasco. 1991. Presence of terminal N-acetylgalactosamine residues in subregions of the endoplasmic reticulum is influenced by cell differentiation in culture. *J. Biol. Chem.* 266:23967–23976.

Preisinger, C., and F.A. Barr. 2005. Kinases regulating Golgi apparatus structure and function. *Biochem. Soc. Symp.* 2005:15–30.

Preisinger, C., B. Short, V. De Corte, E. Bruyneel, A. Haas, R. Kopajtich, J. Gettemans, and F.A. Barr. 2004. YSK1 is activated by the Golgi matrix protein GM130 and plays a role in cell migration through its substrate 14-3-3zeta. *J. Cell Biol.* 164:1009–1020. doi:10.1083/jcb.200310061

Pulvirenti, T., M. Giannotta, M. Capestrano, M. Capitani, A. Pisanu, R.S. Polishchuk, E. San Pietro, G.V. Beznoussenko, A.A. Mironov, G. Turacchio, et al. 2008. A traffic-activated Golgi-based signalling circuit coordinates the secretory pathway. *Nat. Cell Biol.* 10:912–922. doi:10.1038/ncb1751

Quatela, S.E., and M.R. Philips. 2006. Ras signaling on the Golgi. *Curr. Opin. Cell Biol.* 18:162–167. doi:10.1016/j.ceb.2006.02.004

Roskoski, R. Jr. 2004. Src protein-tyrosine kinase structure and regulation. *Biochem. Biophys. Res. Commun.* 324:1155–1164. doi:10.1016/j.bbrc.2004.09.171

Roth, J., Y. Wang, A.E. Eckhardt, and R.L. Hill. 1994. Subcellular localization of the UDP-N-acetyl-D-galactosamine:polypeptide N-acetylgalactosaminyltransferase-mediated O-glycosylation reaction in the submaxillary gland. *Proc. Natl. Acad. Sci. USA*. 91:8935–8939. doi:10.1073/pnas.91.19.8935

Röttger, S., J. White, H.H. Wandall, J.C. Olivo, A. Stark, E.P. Bennett, C. Whitehouse, E.G. Berger, H. Clausen, and T. Nilsson. 1998. Localization of three human polypeptide GalNAc-transferases in HeLa cells suggests initiation of O-linked glycosylation throughout the Golgi apparatus. *J. Cell Sci.* 111:45–60.

Sanchez, J.F., J. Lescar, V. Chazalet, A. Audfray, J. Gagnon, R. Alvarez, C. Breton, A. Imberty, and E.P. Mitchell. 2006. Biochemical and structural analysis of Helix pomatia agglutinin. A hexameric lectin with a novel fold. *J. Biol. Chem.* 281:20171–20180. doi:10.1074/jbc.M603452200

Schwientek, T., E.P. Bennett, C. Flores, J. Thacker, M. Hollmann, C.A. Reis, J. Behrens, U. Mandel, B. Keck, M.A. Schäfer, et al. 2002. Functional conservation of subfamilies of putative UDP-N-acetylgalactosamine:polypeptide N-acetylgalactosaminyltransferases in *Drosophila*, *Caenorhabditis elegans*, and mammals. One subfamily composed of l(2)35Aa is essential in *Drosophila*. *J. Biol. Chem.* 277:22623–22638. doi:10.1074/jbc.M202684200

Spiro, R.G. 2002. Protein glycosylation: nature, distribution, enzymatic formation, and disease implications of glycopeptide bonds. *Glycobiology.* 12:43R–56R. doi:10.1093/glycob/12.4.43R

Tarp, M.A., and H. Clausen. 2008. Mucin-type O-glycosylation and its potential use in drug and vaccine development. *Biochim. Biophys. Acta.* 1780:546–563.

Ten Hagen, K.G., T.A. Fritz, and L.A. Tabak. 2003. All in the family: the UDP-GalNAc:polypeptide N-acetylgalactosaminyltransferases. *Glycobiology.* 13:1R–16R. doi:10.1093/glycob/cwg007

Tenno, M., K. Ohtsubo, F.K. Hagen, D. Ditto, A. Zarbock, P. Schaerli, U.H. von Andrian, K. Ley, D. Le, L.A. Tabak, and J.D. Marth. 2007. Initiation of protein O glycosylation by the polypeptide GalNAcT-1 in vascular biology and humoral immunity. *Mol. Cell. Biol.* 27:8783–8796. doi:10.1128/MCB.01204-07

Thomas, S.M., and J.S. Brugge. 1997. Cellular functions regulated by Src family kinases. *Annu. Rev. Cell Dev. Biol.* 13:513–609. doi:10.1146/annurev.cellbio.13.1.513

Tian, E., and K.G. Ten Hagen. 2009. Recent insights into the biological roles of mucin-type O-glycosylation. *Glycoconj. J.* 26:325–334. doi:10.1007/s10719-008-9162-4

Tooze, S.A., J. Tooze, and G. Warren. 1988. Site of addition of N-acetyl-galactosamine to the E1 glycoprotein of mouse hepatitis virus-A59. *J. Cell Biol.* 106:1475–1487. doi:10.1083/jcb.106.5.1475

Van Lint, J., A. Rykx, Y. Maeda, T. Vantus, S. Sturany, V. Malhotra, J.R. Vandenheede, and T. Seufferlein. 2002. Protein kinase D: an intracellular traffic regulator on the move. *Trends Cell Biol.* 12:193–200. doi:10.1016/S0962-8924(02)02262-6

Wandall, H.H., F. Irazoqui, M.A. Tarp, E.P. Bennett, U. Mandel, H. Takeuchi, K. Kato, T. Irimura, G. Suryanarayanan, M.A. Hollingsworth, and H. Clausen. 2007. The lectin domains of polypeptide GalNAc-transferases exhibit carbohydrate-binding specificity for GalNAc: lectin binding to GalNAc-glycopeptide substrates is required for high density GalNAc-O-glycosylation. *Glycobiology.* 17:374–387. doi:10.1093/glycob/cwl082

Wu, Y.M., D.D. Nowack, G.S. Omenn, and B.B. Haab. 2009. Mucin glycosylation is altered by pro-inflammatory signaling in pancreatic-cancer cells. *J. Proteome Res.* 8:1876–1886. doi:10.1021/pr8008379

Yeatman, T.J. 2004. A renaissance for SRC. *Nat. Rev. Cancer.* 4:470–480. doi:10.1038/nrc1366

Zhang, L., Y. Zhang, and K.G. Hagen. 2008. A mucin-type O-glycosyltransferase modulates cell adhesion during *Drosophila* development. *J. Biol. Chem.* 283:34076–34086. doi:10.1074/jbc.M804267200